

MERRA - NASA's Modern-Era Retrospective Analysis for Research and Applications

Michele M. Rienecker^{1†}, Max J. Suarez¹, Ronald Gelaro¹, Ricardo Todling¹, Julio Bacmeister^{1,2,*}, Emily Liu^{1,3}, Michael G. Bosilovich¹, Siegfried D. Schubert¹, Lawrence Takacs^{1,3}, Gi-Kong Kim¹, Stephen Bloom^{1,3}, Junye Chen^{1,4}, Douglas Collins^{1,3}, Austin Conaty^{1,3}, Arlindo da Silva¹, Wei Gu^{1,3}, Joanna Joiner⁵, Randal D. Koster¹, Robert Lucchesi^{1,3}, Andrea Molod^{1,2}, Tommy Owens^{1,3}, Steven Pawson¹, Philip Pegion^{1,3,#}, Christopher R. Redder^{1,3}, Rolf Reichle¹, Franklin R. Robertson⁶, Albert G. Ruddick^{1,3}, Meta Sienkiewicz^{1,3}, Jack Woollen⁷

Submitted to *Journal of Climate* (MERRA Special Collection)

¹Global Modeling and Assimilation Office, NASA Goddard Space Flight Center, Greenbelt, Maryland, USA

²Goddard Earth Sciences and Technology Center, University of Maryland, Baltimore County, Baltimore, MD, USA

³Science Applications International Corporation, Beltsville, Maryland, USA

⁴Earth System Sciences Interdisciplinary Center, University of Maryland, College Park, MD, USA

⁵Atmospheric Chemistry and Dynamics Branch, NASA Goddard Space Flight Center, Greenbelt, Maryland, USA

⁶NASA Marshall Space Flight Center, Huntsville, AL, USA

⁷NOAA, National Centers for Environmental Prediction, Camp Springs, MD, USA

*Now at National Center for Atmospheric Research, Boulder, Colorado, USA

#Now at NOAA/Earth Systems Resource Laboratory, Boulder, Colorado, USA

†*Corresponding address*: Global Modeling and Assimilation Office, Code 610.1, NASA / Goddard Space Flight Center, Greenbelt, MD 20771, Michele.M.Rienecker@nasa.gov

Abstract

The Modern-Era Retrospective analysis for Research and Applications (MERRA) was undertaken by NASA's Global Modeling and Assimilation Office with two primary objectives: to place observations from NASA's Earth Observing System satellites in a climate context, and to improve upon the hydrologic cycle represented in earlier generations of reanalyses. Focusing on the satellite era, from 1979 to the present, MERRA has achieved its goals with significant improvements in precipitation and water vapor climatology. Here, we give a brief overview of the system and some aspects of its performance, and introduce new quality assessment diagnostics, such as *contextual bias*, from innovation and residual statistics.

By comparing MERRA with other updated reanalyses (ERA-Interim and the Climate Forecasting System Reanalysis (CFSR)), we identify advances made in this new generation of reanalyses, as well as remaining deficiencies. Although there is little difference between the new reanalyses in many aspects of climate variability, substantial differences remain in poorly constrained quantities such as precipitation and surface fluxes. These differences, due to differences both in models and in analysis techniques, are an important measure of the uncertainty in reanalysis products. We also find that all reanalyses are still quite sensitive to observing system changes. Dealing with this sensitivity remains the most pressing challenge for the next generation of reanalyses.

MERRA production has now caught up to the present and is being continued as a near-real-time climate analysis. The output is available online through the NASA Goddard Earth Sciences Data and Information Services Center (GES DISC).

1. Introduction

Reanalyses combine model fields with observations distributed irregularly in space and time into a spatially complete gridded meteorological data set, with an unchanging model and analysis system spanning the historical data record. The earlier generations of reanalyses from NOAA's National Centers for Environmental Prediction (NCEP), the European Center for Medium Range Weather Forecasting (ECMWF), and the Japan Meteorological Agency (JMA) (e.g., Kalnay et al. 1996; Uppala et al. 2005; Onogi et al. 2005) have proven to be extremely valuable scientific tools, enabling climate and weather research not otherwise possible. They continue to be used, even with their known limitations, because of the basic utility afforded by such data sets for scientific analysis.

The Modern-Era Retrospective analysis for Research and Application (MERRA) was stimulated by the recognition that various aspects of the hydrologic cycle represented in previous generations of reanalyses were not adequate for climate and weather studies. MERRA proposed to improve upon the water cycle as a contribution to the science community and reanalysis research. MERRA's span of most of the satellite era is also intended to place observations from NASA's Earth Observing System (EOS) satellites, particularly those available since October 2002 from EOS/Aqua, in a climate context.

MERRA was generated with the Goddard Earth Observing System (GEOS) atmospheric model and data assimilation system (DAS), version 5.2.0. The system, the input data streams and their sources, and the observation and background error statistics are documented fully in Rienecker et al. (2008, henceforth R2008). Unlike the atmospheric reanalyses from centers focused on operational weather prediction, the GEOS atmospheric DAS was developed with NASA instrument teams and science community as the primary customers. Hence, the performance drivers of the GEOS DAS products have historically been temperature and moisture fields suitable for the EOS instrument teams, wind fields for the transport studies by the stratospheric and tropospheric chemistry communities, and climate-quality analyses (Schubert et al. 1993). With MERRA in particular, the aim has been to support the broader community of reanalysis users and, in doing so, to make the products readily accessible by serving them online.

This paper provides an introduction to MERRA for a series of papers that evaluate the MERRA products and their use in particular scientific investigations. It summarizes the DAS and provides some technical details as well as some insight into system performance. Other papers in the series analyze various aspects of the scientific quality of MERRA. For example, Bosilovich et al. (2011) evaluates MERRA from an energy and water budget perspective; Robertson et al. (2011) analyzes the effect of the changing observing system on MERRA's energy and water fluxes; Schubert et al. (2011) highlights the usefulness of MERRA for characterizing the nature and forcing of short-term climate extremes, such as heat waves and flooding events, and Cullather et al. (2011a, b) evaluates MERRA surface fields in the polar regions. Pawson et al. (2011) looks at the impacts of the changing observing system on MERRA in the stratosphere. Reichle et al. (2011) evaluates MERRA land surface hydrological fields in offline tests and introduces a supplemental and improved set of fields. Yi et al. (2011) and Decker et al. (2011) evaluate surface meteorological forcing fields and surface fluxes over land from MERRA and other reanalyses with satellite estimates and in situ observations from flux towers. Roberts et al. (2011) and Brunke et al. (2011) analyze surface turbulent fluxes over the ocean from MERRA and other data products. Harnik et al. (2011) uses MERRA to analyze decadal changes in downward wave coupling between the stratosphere and troposphere. By identifying both strengths and weaknesses of the products, research efforts such as these provide valuable feedback that can improve future reanalyses.

Section 2 summarizes the DAS and processing strategy for MERRA. Section 3 summarizes the observations used and provides some details on the processing of radiosondes and satellite radiances. An evaluation of the status of the spin-up for several fields is provided in Section 4. Innovation statistics as one measure of the quality of MERRA are discussed in Section 5, which also introduces new statistical analyses that can be used to provide quality measures and insight into how the different observations contribute to the analyses. Sections 6, 7, and 8 provide a view of how MERRA and other recent reanalyses have improved upon earlier generations. Remaining challenges are also discussed. Section 9 provides information about MERRA products and how they can be accessed. Finally, Section 10 looks ahead to the next generation of reanalyses.

2. The MERRA System and Production

a. The GEOS-5 Data Assimilation System

The GEOS-5 atmospheric general circulation model (AGCM) used for MERRA is based on finite-volume dynamics (Lin 2004) found to be effective for transport in the stratosphere (e.g., Pawson et al. 2007). It includes moist physics with prognostic clouds (Bacmeister et al. 2006), a modified version of the Relaxed Arakawa-Schubert convective scheme described by Moorthi and Suarez (1992), the shortwave radiation scheme of Chou and Suarez (1999), and the long-wave radiation scheme of Chou et al. (2001). Two atmospheric boundary-layer turbulent mixing schemes are used. The Louis et al. (1982) scheme is used in stable situations with no planetary boundary layer (PBL) clouds, while the Lock et al. (2000) scheme is used for unstable or cloud-topped PBLs. GEOS-5 incorporates both an orographic gravity wave drag scheme based on McFarlane (1987), and a scheme for non-orographic waves based on Garcia and Boville (1994). The land surface is modeled with the Catchment Land Surface Model (Koster et al. 2000). The grid used for MERRA is $\frac{1}{2}^\circ$ latitude \times $2/3^\circ$ longitude with 72 vertical levels, from the surface to 0.01 hPa. Additional details are provided in R2008.

MERRA uses a three-dimensional variational (3D-Var) analysis algorithm based on the Grid-point Statistical Interpolation scheme (GSI, Wu et al. 2002, Derber et al. 2003, Purser et al. 2003a,b) with a six-hour update cycle. The GSI, originally developed at NCEP and now jointly developed by NCEP and the GMAO, includes a number of advancements over 3D-Var algorithms used previously. In particular, the observation-minus-background departures are computed with increased temporal accuracy, and a dynamic constraint on noise is employed to improve the balance properties of the analysis solution. Unlike CFSR, which also uses the GSI, GEOS-5 uses an incremental analysis update (IAU) procedure (Bloom et al. 1996) in which the analysis correction is applied to the forecast model gradually, through an additional tendency term in the model equations during the corrector segment (Figure 1). This has ameliorated the spin-down problem with precipitation during the very early stages of the forecast and greatly improved aspects of the stratospheric circulation.

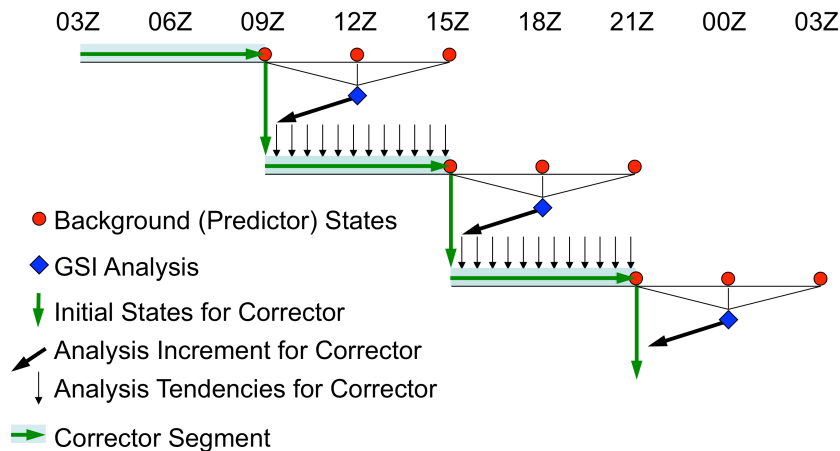


Figure 1: A schematic of the IAU implementation in GEOS-5.

MERRA, like other current reanalyses, makes extensive use of satellite radiance information, including data from hyper-spectral instruments such as the Atmospheric Infrared Sounder (AIRS) on Aqua. The assimilation of radiance data requires a forward radiative transfer model as the observation operator, to calculate the model-equivalent radiances, and the corresponding Jacobian to calculate the influences in model space of the radiance increments calculated from the analysis. For this, the GSI is coupled to the Community Radiative Transfer Model (CRTM, Han et al. 2006). The CRTM was used for all radiance data except the Stratospheric Sounding Unit (SSU). The forward model for SSU has to take into account a leaking problem in the instrument's CO₂ cell pressure modulator that caused the radiances from each satellite to drift in time (Kobayashi et al. 2009). Since this information was not available in the CRTM at the time of MERRA development, the radiative transfer calculations for the SSU used an external module that incorporated the cell pressure information and was integrated into the GSI outside the CRTM. Shine et al. (2008) shows that the SSU spectral weighting functions are also sensitive to changes in atmospheric CO₂ concentrations, however this information was not included in the forward model used for MERRA.

Since no land surface analysis was attempted, MERRA land surface estimates reflect the Catchment model's time integration of the surface meteorological conditions (precipitation, radiation, wind speed, etc) generated by the AGCM during the corrector segment.

b. Boundary and ancillary data

Unlike more recent versions of the GEOS-5 system, the MERRA AGCM uses a climatological aerosol distribution generated using the Goddard Chemistry, Aerosol, Radiation, and Transport (GOCART) model with transport based on a previous (GEOS-4) version of the AGCM (Colarco et al. 2010). The MERRA AGCM does, however, use the analyzed ozone generated by the DAS. The sea surface temperature and sea ice concentration boundary conditions are derived from the weekly 1° sea surface temperature product of Reynolds et al. (2002), linearly interpolated in time to each model time-step. The MERRA system also nudges the stratospheric water vapor to zonal mean climatological values based on data from the Halogen Occultation Experiment (HALOE, Randel et al. 1998) and the Microwave Limb Sounder (MLS) on the Aura satellite.

c. Production

MERRA was processed in three separate streams, each spun-up in two stages: a two-year analysis at 2° × 2.5° and then a one-year analysis on the MERRA grid. Unfortunately, some system changes were made between spin-up and production; these included small changes to the model that should have had little impact on the analysis, but also updates to spectral coefficients used in the CRTM and a correction to quality control of microwave observations. Since the spin-up was primarily aimed at the root-zone soil moisture, it was felt that these changes would not impede spin-up. However, Streams 1 and 2 were each extended to overlap the next stream so that the overlaps could be used to examine the adequacy of the spin-up procedure and to quantify the uncertainty in individual fields. The adequacy of the spin-up is discussed in Section 4. The final MERRA distribution is from Stream 1 for 1 January 1979 to 31 December 1992,

followed by Stream 2 for 1 January 1993 to 31 December 2000, and then continues with Stream 3 for 1 January 2001 to the present. Hence, the distributed product segments from Streams 1, 2 and 3 have been spun up for zero, four and three years, respectively, at MERRA resolution with the precise MERRA system configuration (Figure 2). With the overlaps complete, and Stream 3 now at “the present”, data production is being continued as a near-real-time climate analysis from Stream 3 alone.

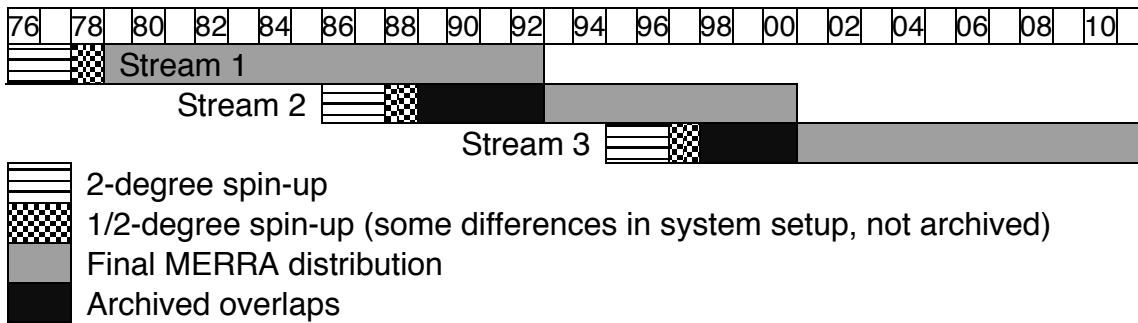


Figure 2: The MERRA streams, showing the original spin-ups, the overlaps, and the final MERRA distribution.

3. Observations

The various data types used in MERRA and the timeline of their availability are summarized in Figure 3. The complete listing of the data streams and their sources are provided in Appendix A. The quality control procedures, the channels used for radiance assimilation, and the observation error characteristics are presented in R2008.

MERRA benefited from the observational assembly for the NCEP/NCAR reanalysis version 1, the NCEP preparations for its latest reanalysis, the CFSR (Saha et al. 2010), and also advances made for ERA-Interim (Dee and Uppala 2009, henceforth DU09). While the data sets used in MERRA, ERA-Interim and CFSR are, to a large extent, similar, there are some known differences in the observations and their processing, as mentioned below. Obviously, these differences can be one source of difference between the various reanalysis products; others sources are the model and the analysis methods that were used.

Figure 4a shows the total number of observations available for assimilation and their breakdown by instrument or type. A large increase in the number of observations is seen with the availability of the Advanced TIROS Operational Vertical Sounder (ATOVS) in 1998, and then again with the availability of AIRS and the Advanced Microwave Sounding Unit-A (AMSU-A) on the Aqua satellite in 2002. After 2002, roughly 4 million observations are considered in each six-hour analysis cycle, with roughly half of these being assimilated (Figure 4b) because of quality control checks as well as data-thinning.

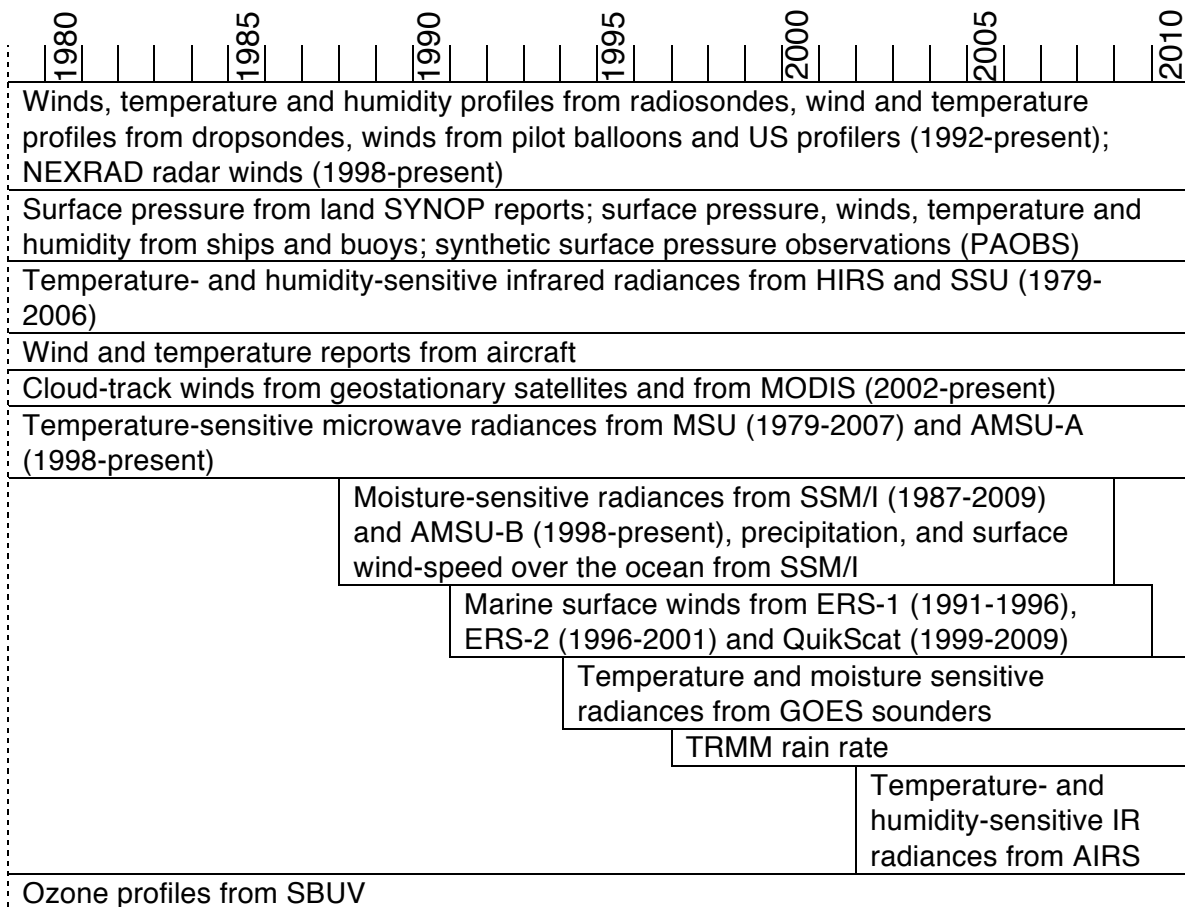


Figure 3: Summary of the observing system used for MERRA.

a. Conventional Observations

Conventional observations consist of measurements of standard atmospheric variables (i.e. pressure, temperature, height, wind components) taken by instrumentation on weather stations, balloons, aircraft, ships, buoys, and satellites. A fairly complete global coverage of these observations has been available since roughly the late 1940's. Archives of conventional observations were preserved among a number of national, academic, and military sources worldwide. Institutions such as the National Center for Atmospheric Research (NCAR) and the National Climatic Data Center (NCDC) have collected and converted many of the original archives into digital formats compatible with modern data processing systems. In order to produce homogeneous sets of observations for use in reanalysis, it is necessary to combine observations from the different sources, eliminating redundant information in the process. This was done for all the conventional data types listed above. Figure 4c illustrates the number radiosonde soundings per year from each major source archive represented in the composited set of radiosondes produced for reanalysis, 1948-2000. An itemization of all source files from each archive location for each conventional data type is given in Appendix A.

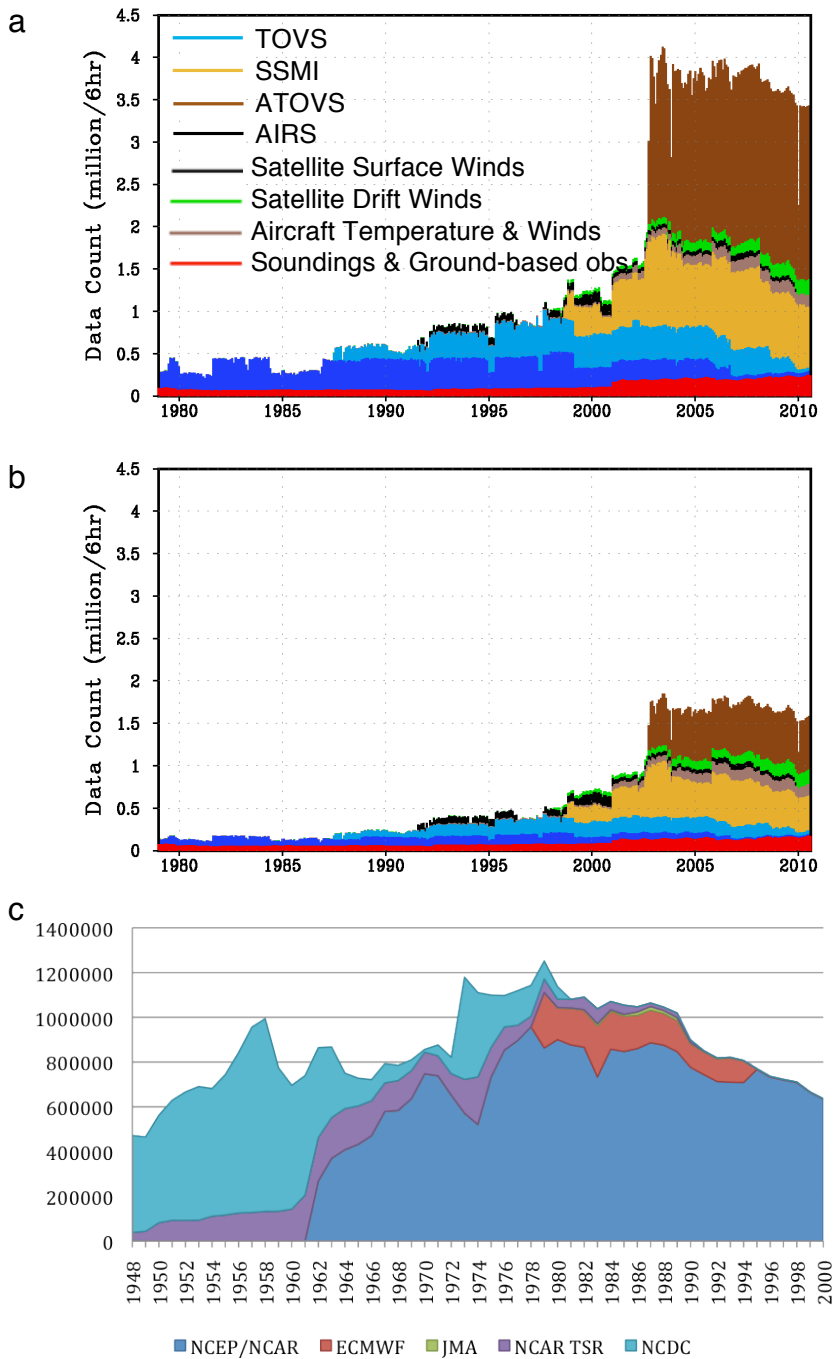


Figure 4: Time series of (a) the number (millions) and types of observations considered for assimilation during a 6-hour window, and (b) those observations actually assimilated. (c) Counts of merged radiosonde soundings per year from each major archive source, 1948-2000.

Radiosonde data remain some of the most important observations for meteorological analyses. MERRA used radiosonde data that were quality-controlled by NCEP for CFSR, with additional processing and correction of the data undertaken at GMAO. Corrections included the removal of large time-mean temperature differences in radiosonde observations collected at 00 and 12 UTC with the Vaisala RS-80 instrument. The

differences occur as a result of a coding error in the post-processing software at the observing stations, and primarily affect observations in the stratosphere (Redder et al. 2004). Reported elapsed time archived in the NCDC database was used to undertake the corrections. The homogenization scheme of Haimberger (2007) (Radiosonde Observation Bias Correction Using Reanalysis, RAOBCORE v1.4) was then applied to radiosonde observations until 2005, with updated values consistent with the Vaisala RS-80 corrections. After these corrections were made to the radiosonde temperature observations, a radiation bias correction was applied to account for seasonal changes in the solar elevation angle that affect the thermistor. For assimilation, the ERA-40 blacklist was used. The other conventional observations used for MERRA are listed in Table A.1.

b. Satellite radiance data and variational bias correction

MERRA, like other current reanalyses, makes extensive use of satellite radiance data from both operational and research instruments. Successful use of radiance data requires careful quality control and bias correction procedures that are channel-specific. The bias in a given satellite channel can vary significantly in space and time depending on atmospheric conditions, systematic errors in the radiative transfer model, and quality and age of the instrument. In most data assimilation schemes, the bias in each satellite radiance measurement is represented by a linear predictor model with a relatively small number (~10) of parameters. In the earlier reanalyses that used satellite radiances, including ERA-40 (Uppala et al. 2005) and the Japanese 25-yr Reanalysis (JRA-25, Onogi et al. 2005), these parameters were estimated separately for each channel using an offline procedure based on a reference data set.

In the current reanalyses, bias estimation is performed automatically during the data assimilation procedure using a variational bias correction scheme (VBC, Derber and Wu 1998; Dee 2005). The bias parameters are updated during each analysis cycle by including them in the control vector used to minimize the analysis cost function. This ensures that the bias estimates are continuously adjusted to maintain consistency of the bias-corrected radiances with all other information used in the analysis, including conventional observations and the model background state. An important technical advantage of this approach is that it removes the need for manual tuning and other interventions as the satellite observing system changes over time. The bias estimates also adapt in response to natural phenomena that can severely affect the radiance measurements, such as the Mt. Pinatubo eruption in 1991 (see Figure 5 in DU09). The use of VBC thus represents one of the most important advances in the assimilation methodology of the current generation of reanalyses. The linear predictors used in the GSI differ slightly from those used for ERA-Interim and are documented in R2008.

Not all instrument channels can be bias-corrected using the assimilation machinery of VBC. The success of such corrections depends entirely on having either an AGCM with low biases or other observations with low biases to provide an anchor for the analysis. Since models tend to have large biases in the upper stratosphere and mesosphere, and there are no observations consistently available over the entire reanalysis period, bias-correction for instrument channels with weighting functions that extend above about 2 hPa is problematic.

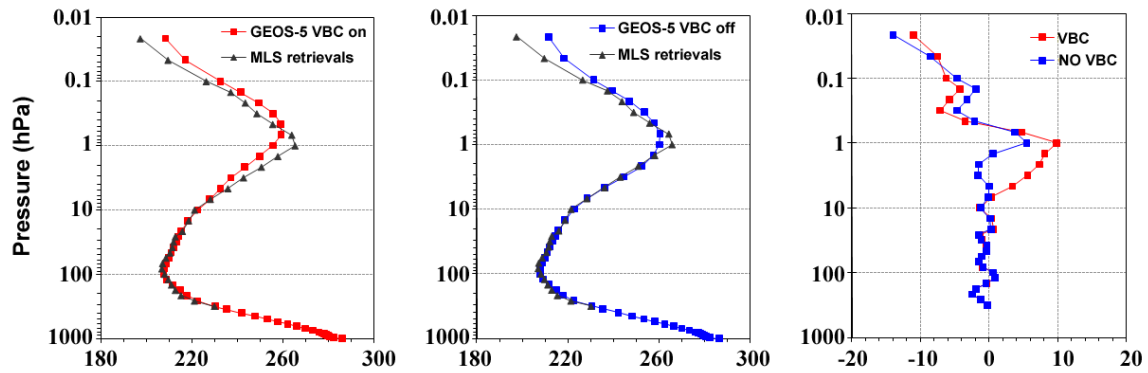


Figure 5: Mean temperature profiles (K) from MLS and collocated MERRA profiles over the globe for August 2008. The left-hand panel shows the comparison when variational bias correction (VBC) is applied to AMSU-A Channel 14. The center panel shows the comparison without VBC. The right-hand panel displays the differences between the mean profiles for each case.

An evaluation of the MERRA temperature fields in the upper stratosphere, as well as the impact of trying to bias-correct those high-peaking channels is provided by a comparison with temperature data from MLS (Figure 5). MLS provides detailed temperature structure from about 316 hPa to about 0.001 hPa (e.g., Manney et al. 2008a). These data were not assimilated in MERRA, providing independent validation. For the comparison shown in Figure 5, approximately 95,000 MLS profiles were collocated to the MERRA grid during August 2008. The right-hand panel shows that the analysis has a cold bias of up to 10 K from about 10 hPa to 0.8 hPa when VBC was activated for Channel 14 on the AMSU-A. Without VBC, this channel effectively corrects the model bias, which is responsible for the analysis bias when VBC is activated. Accordingly, in MERRA, VBC is not applied to AMSU-A Channel 14 or SSU Channel 3 (which peaks at a similar level, about 1.5 hPa, Kobayashi et al. 2009). However, biases of up to 5 K are still evident at 1 hPa and above.

Just as variational bias correction has provided significant benefit to the assimilation of satellite radiances, so too has the cross-calibration of certain observation data sets improved their usefulness in the current reanalyses. The Microwave Sounding Unit (MSU) instruments on board TIROS-N and the NOAA series to NOAA-14 provide one of the longest records of remotely sensed atmospheric temperature from a single sensor type, extending from 1978 to 2007, with overlapping lifetimes of up to three years between satellites. In the original data sets, the global mean bias estimates for the same MSU channel on different satellites differ by up to 1 K or more (DU09), limiting the usefulness of these data for climate-change research and possibly having a negative effect in the variational bias correction scheme. The National Environmental Satellite, Data, and Information Service (NESDIS) has begun recalibrating observations from MSU as well as other instruments using a simultaneous nadir overpass (SNO, e.g., Zou et al. 2006) method. The recalibrated radiances for MSU channels 2 – 4 on board NOAA-10, -11, -12 and -14 have been assimilated in MERRA and exhibit near-uniform biases, albeit with a

discernible trend over the first few years the data record (Figure 6). The bias estimates shown here may be compared with those of the uncalibrated radiances used in ERA-Interim (DU09, Figure 3). Zou et al. (2006) estimate the new global ocean-averaged inter-satellite biases for channel 2 to be between 0.05 to 0.1 K. The VBC procedure used in MERRA, which includes all other available observations as well as information from the model background state, produces a slightly higher estimate of about 0.25 K, which is still much smaller than the ~ 1.5 K inter-satellite bias from the raw measurement (DU09). Note that it has not been determined yet whether cross-calibration affects the quality of the reanalysis product, but it is reasonable to speculate that it is beneficial to the performance of the VBC.

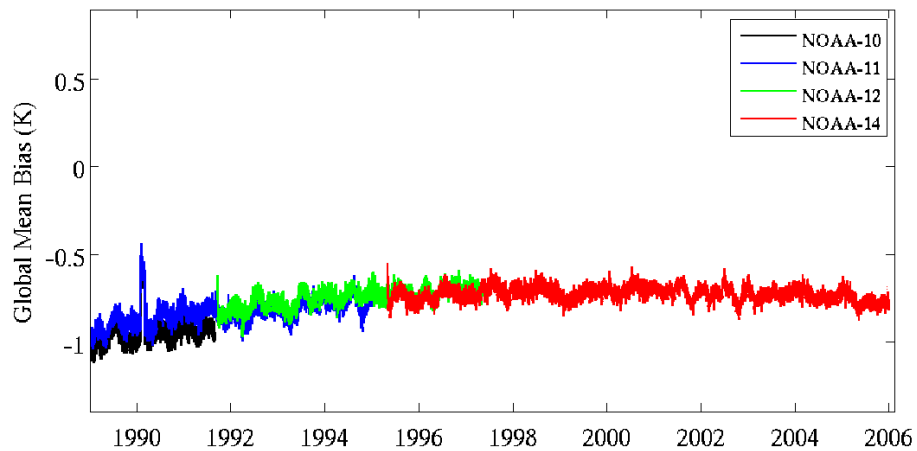


Figure 6: Time series of MERRA's global mean 6-hourly variational bias estimates (K) for cross-calibrated MSU channel 2 radiance data from NOAA-10, -11, -12, and -14.

4. Evaluation of the Spin-up

The primary fields for which spin-up of the assimilation system is a concern are the land surface states and the stratosphere. The spin up of the stratosphere is addressed in Pawson et al. (2011); here we examine the troposphere, the land surface states, and precipitation. The tropospheric meteorological fields (as assessed by the root-mean-square (RMS) difference in 500 hPa height during the overlap periods) reached a steady state after about 1.5 years of spin-up with the final MERRA configuration (Figure 7a). Precipitation takes slightly longer, about two years (Figure 7b). These initial adjustments are very small compared with the uncertainties in these quantities (see, e.g., the MERRA atlas described in Section 9).

Subsurface properties, such as the root-zone soil wetness shown in Figure 8, reach their asymptote slightly more slowly, after a sharp drop in differences over the first six months of the overlap using the same model parameters (from 1 January 1989 in Stream 2, Figure 8). Although the RMS differences in the Northern Hemisphere are still diminishing after four years, they appear to reach a predictability limit, especially in the tropics and Southern Hemisphere where the RMS differences also display some seasonality. This seasonality appears to be related to corresponding seasonality in the RMS differences in precipitation (not shown), presumably, in turn, related to the seasonal cycle of

precipitation over tropical land. The maps of root zone soil wetness differences for February (Figure 9) show that the slowly decaying systematic differences tend to be in the high latitudes, where adjustments to soil moisture by evaporation or runoff cannot occur over long periods of the year because of frozen conditions.

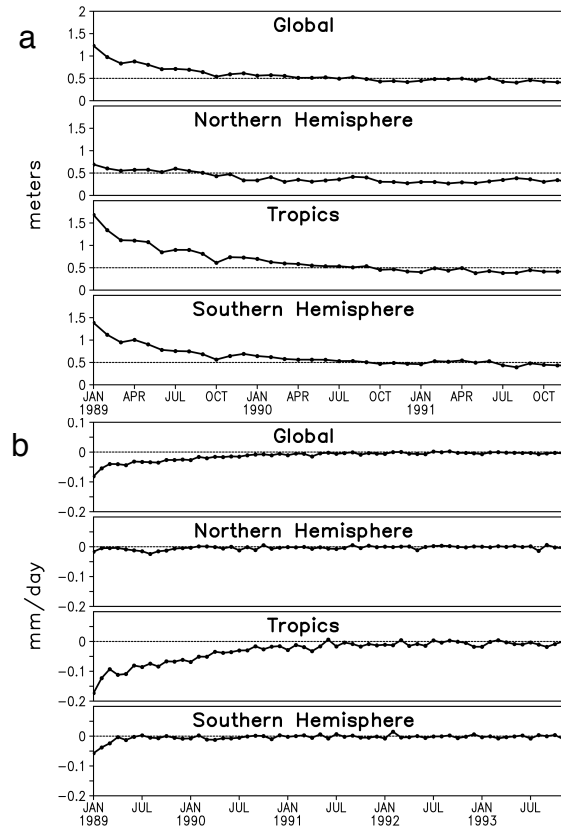


Figure 7: Time series of (a) RMS difference in monthly mean 500 hPa height (m) and (b) difference in monthly mean precipitation (mm day^{-1}) from the overlap of Stream 1 and 2. Stream 2 was initialized at the MERRA resolution in January 1988 after a 2-year spin-up on a $2^\circ \times 2.5^\circ$ grid. The tropical band covers 15°S to 15°N .

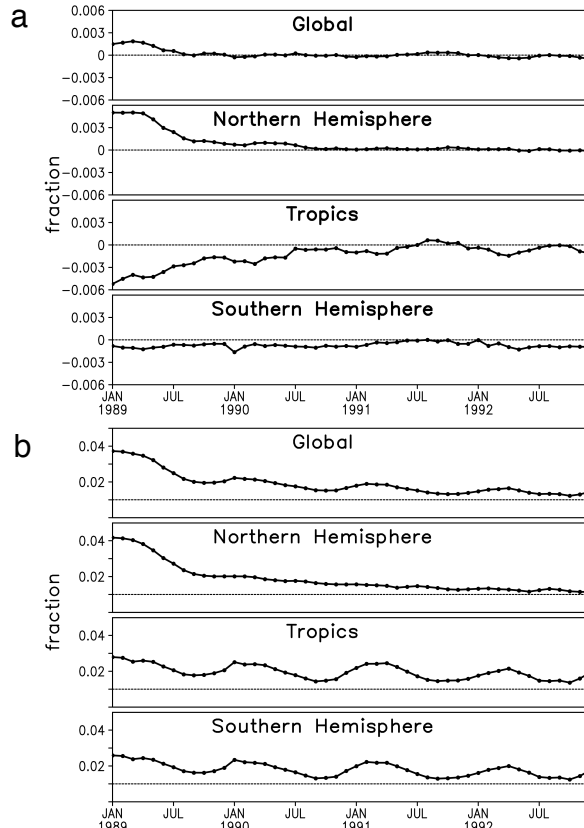


Figure 8: Time series of the (a) mean and (b) RMS difference between Stream 1 and Stream 2 for monthly mean root-zone soil wetness (dimensionless fraction of saturated conditions, varying from 0 to 1). The tropical band covers 15°S to 15°N.

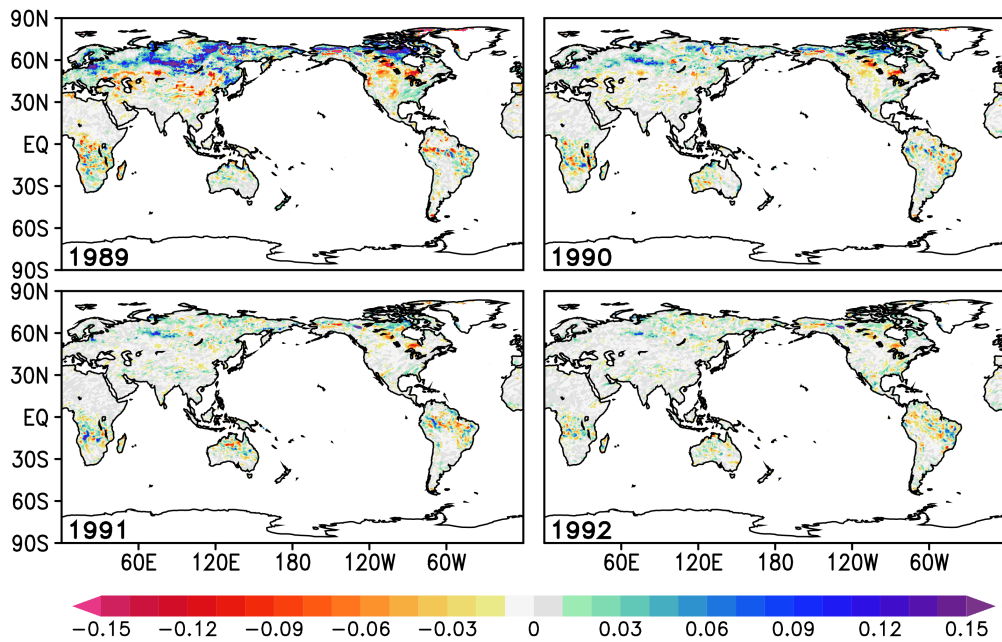


Figure 9: The monthly mean difference between the root-zone soil wetness, Stream 1 minus Stream 2, for February 1989-1992.

5. Evaluation of MERRA through innovation statistics

The differences between the observations and the forecast background used for the analysis (the innovations or O-F for short) and those between the observations and the final analysis (O-A) are by-products of any assimilation system and provide information about the quality of the analysis and the impact of the observations. Innovations have been traditionally used to diagnose observation, background and analysis errors at observation locations (Hollingsworth and Lönnerberg 1989; Dee and da Silva 1999). At the most simplistic level, innovation variances can be used as an upper bound on background errors, which are, in turn, an upper bound on the analysis errors. With more processing (and the assumption of optimality), the O-F and O-A statistics can be used to estimate observation, background and analysis errors (Desroziers et al. 2005). They can also be used to estimate the systematic and random errors in the analysis fields.

Unfortunately, such data are usually not readily available with reanalysis products. With MERRA, however, a gridded version of the observations and innovations used in the assimilation process is being made available. The dataset allows the user to conveniently perform investigations related to the observing system and to calculate error estimates. Da Silva (2011) provides an overview and analysis of these datasets for MERRA.

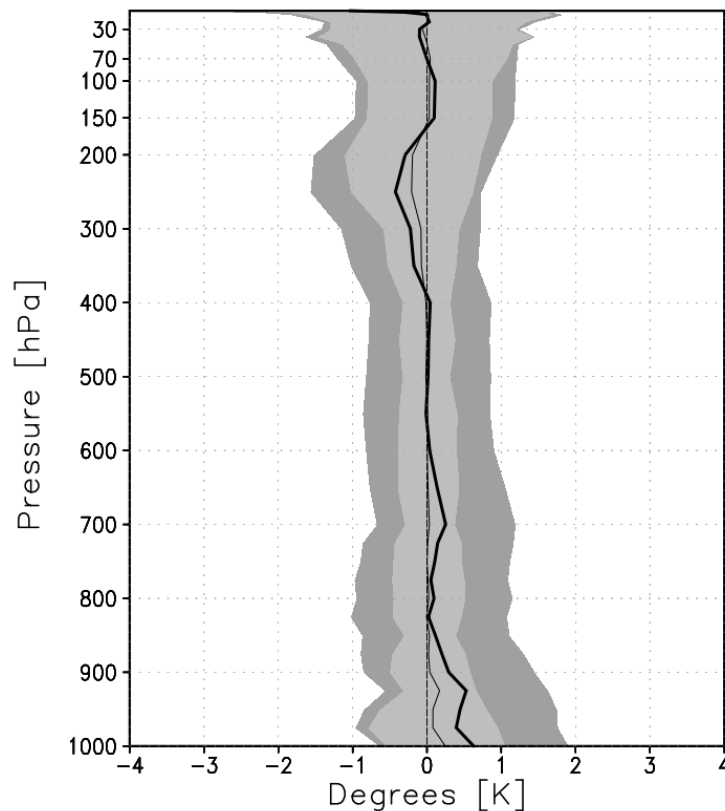


Figure 10: Vertical profile of global mean O-F (thick curve) and O-A (thin curve) residuals (K) for radiosonde temperature observations as a function of pressure level (hPa) during January 2004. The dark and light shading indicate ± 1 standard deviation from the mean O-F and O-A values, respectively.

The global mean O-F and O-A statistics for radiosonde temperature observations at different pressure levels are shown for January 2004 in Figure 10. The biases are

relatively small (less than 0.5 K) at most levels, with a cold bias (positive O-F) in the PBL and a warm bias in the upper troposphere, consistent with the analysis biases against independent MLS observations discussed earlier (Figure 5). Interestingly, these O-F statistics change with time (Figure 11), especially in the upper troposphere. Since in the reanalysis the model does not change and there is no indication of degradation in the radiosonde observations themselves over time, we conclude that other observation types contribute to these changes in the agreement between the analysis (and also the background forecast) and the radiosondes. This issue is explored further in Figure 12. Even before the increase in the bias, there is a decrease in the standard deviation of the radiosonde innovations associated with the decrease in the number of radiosonde observations.

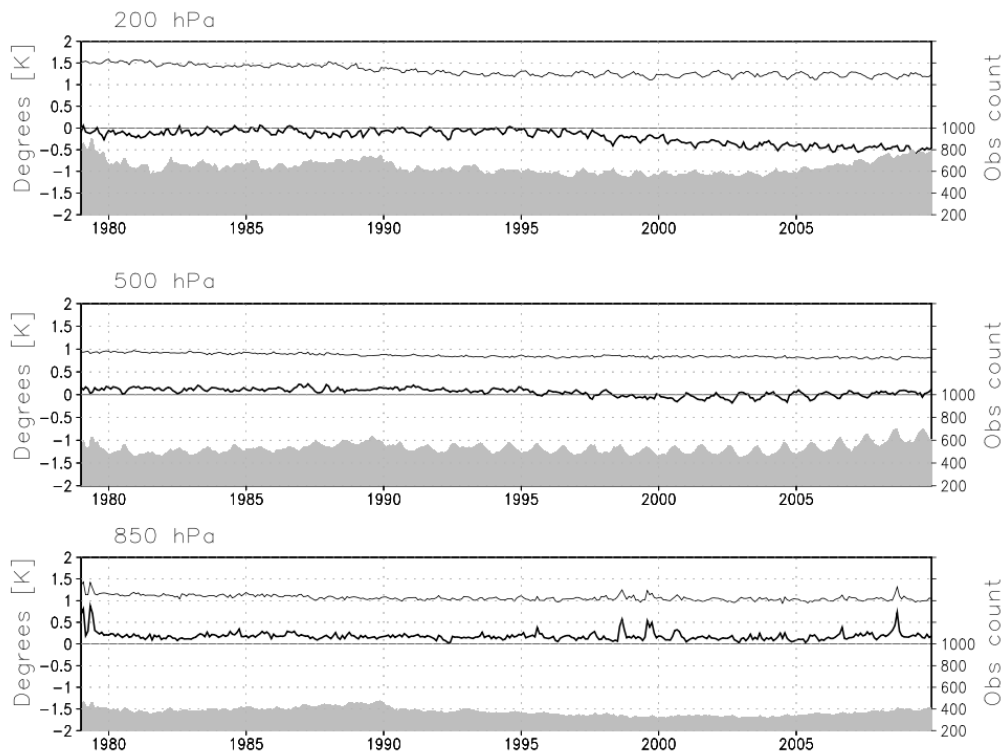


Figure 11: Time series of the monthly global mean (thick curve) and standard deviation (thin curve) of O-F residuals (K, left axis) for radiosonde temperature observations at 200 hPa (top), 500 hPa (middle) and 850 hPa (bottom). Negative mean values indicate that the observations are colder, on average, than the background. The shaded curves indicate the monthly mean data counts (right axis) for each 6-hr assimilation cycle.

Figure 12a shows the time series of monthly innovation statistics for radiosonde temperature at 300 hPa. The thin black line depicts the spatial-temporal mean O-F for each month. Comparison with the same statistic for aircraft temperatures (Figure 12b) shows that the increase in the magnitude of the upper tropospheric bias with respect to radiosondes starting in the mid- to late nineties coincides with an increase in aircraft observations, which have a warm bias (Cardinali et al. 2003, DU09). As pointed out by

DU09, after 1999 the mean analyzed temperatures are increasingly determined by the more numerous aircraft data, especially in the Northern Hemisphere, even though the observation error specified for radiosondes tends to be slightly lower than that specified for aircraft (0.65 K for radiosondes and 0.8K for most aircraft observations at 300 hPa in MERRA).

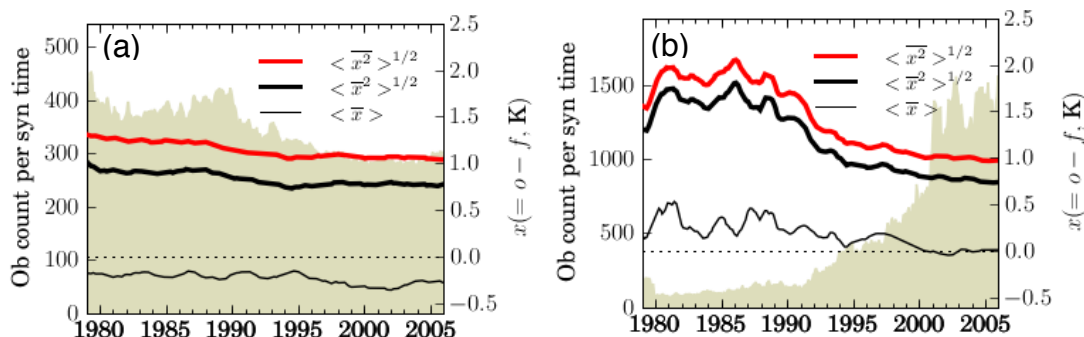


Figure 12: (a) Time series of monthly global mean O-F statistics for radiosonde temperature observations at 300 hPa. The thin black line shows the global-mean (angle brackets) monthly-mean (overbar) difference, the thick black line shows the spatial RMS of the monthly mean, and the red line shows the spatial-time RMS, all in degrees K (right axis). Shading represents the number of observations per synoptic time (left axis). Curves have been smoothed with a 12-month running mean. Panel (b) shows the same statistics for temperature observations at 300 hPa, but taken from aircraft.

Two complementary statistics are also depicted in Figure 12. The thick black line shows the spatial RMS of monthly mean values in each grid box (Da Silva, 2011). This statistic shows the contribution of the spatial variability of the O-F bias, which can be ascribed in part to the instrument inhomogeneities but most likely reflects the large-scale structure of the background bias. The red curve depicts the space-time RMS for each month. The difference between the red and thick black lines offers an indication of the contribution of synoptic scale eddies to the O-F misfit. These statistics indicate that the dominant components of the background error are systematic rather than random.

The innovations may be thought of as the correction to the background required by a given instrument, while the analysis increment (A-F) is the consolidated correction once all instruments, observation errors, and background errors have been taken into consideration. The extent to which the O-F statistics for the various instruments are similar to the A-F statistics reflects the degree of homogeneity of the observing system as a whole. Using the joint probability density function (PDF) of innovations and analysis increments, da Silva (2011) introduces the concepts of the *effective gain* (by analogy with the Kalman gain) and the *contextual bias*. In brief, the effective gain for an observation is a measure of how much the assimilation system has drawn to that type of observation, while the contextual bias is a measure of the degree of agreement between a given observation type and all other observations assimilated. For details of the computation of these quantities and their interpretation, the reader is referred to da Silva (2011).

Figure 13 shows a time series of the contextual bias and effective gain, along with the correlation between O-F and A-F, for radiosonde virtual temperature at 300 hPa. Consistently over the record, about 60% of the innovations are realized as analysis increments, with the O-F and A-F being correlated at 90%. These observations exhibit a larger (more negative) contextual bias in the 1980s and early 1990s, probably due to the influence of data from thermal infrared sensors such as the High resolution Infrared Radiation Sounder (HIRS). This bias decreases more or less steadily with time after 1990, probably due to the influence of higher-quality satellite data available in recent years. Note that this contextual bias reflects the observations themselves, not the bias of the background (as seen in Figure 12), which is influenced by the weights given individual observations in a prior analysis. The fact that the contextual bias of the radiosonde observations at 300 hPa decreases over time is another indication that the increase in background bias relative to radiosondes seen in Figure 12 is due to the influence of other observations (the aircraft data) on the analysis, as inferred above.

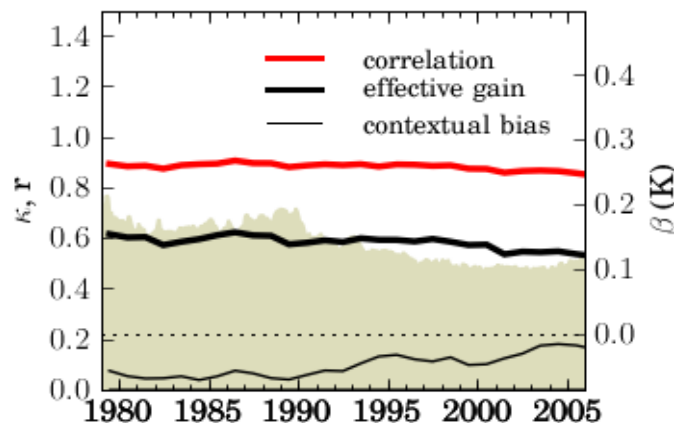


Figure 13: Time series of correlation (red), effective gain (thick black) and contextual bias (thin black) based on radiosonde virtual temperature data at 300 hPa. The axis for correlation and effective gain is on the left; the axis for the contextual bias is on the right.

With MERRA’s gridded observation and innovation data sets, a wealth of information is available for examination of the quality of the analyses and how the different observations impact the analyses and interact with each other. Such examinations can be conducted regionally or globally and should provide useful information for the next generation of reanalyses.

6. Climate Variability

Many aspects of the quality of MERRA products are presented in other papers mentioned in the Introduction. In the next three sections, we touch on just a few fields that highlight improvements over earlier-generation reanalyses and on some of the issues that will still need to be addressed in the next generation.

One of the strengths of the most recent reanalyses is in the representation of interannual variability of the atmospheric state on monthly to seasonal time scales. However, the quality is not uniform, depending on both the variable of interest and the location. Not surprisingly, the interannual variability in analyzed fields, like 500 hPa height (not shown), from different reanalyses in the satellite era is almost indistinguishable. Perhaps more surprising is the agreement in higher order moments, like large-scale atmospheric transports, or in some of the derived fields, like vertical velocity. The latter is illustrated in Figure 14 by comparing results from MERRA and ERA-Interim. The difference in the representation of these climate anomalies, as indicated by the difference between monthly-mean analyses for two different years (one a neutral year in terms of the El Niño-Southern Oscillation (ENSO) and one an El Niño year), is much smaller than the amplitude of the El Niño climate signal itself. This agreement is an improvement upon what was already a high level of agreement with the older ERA-40.

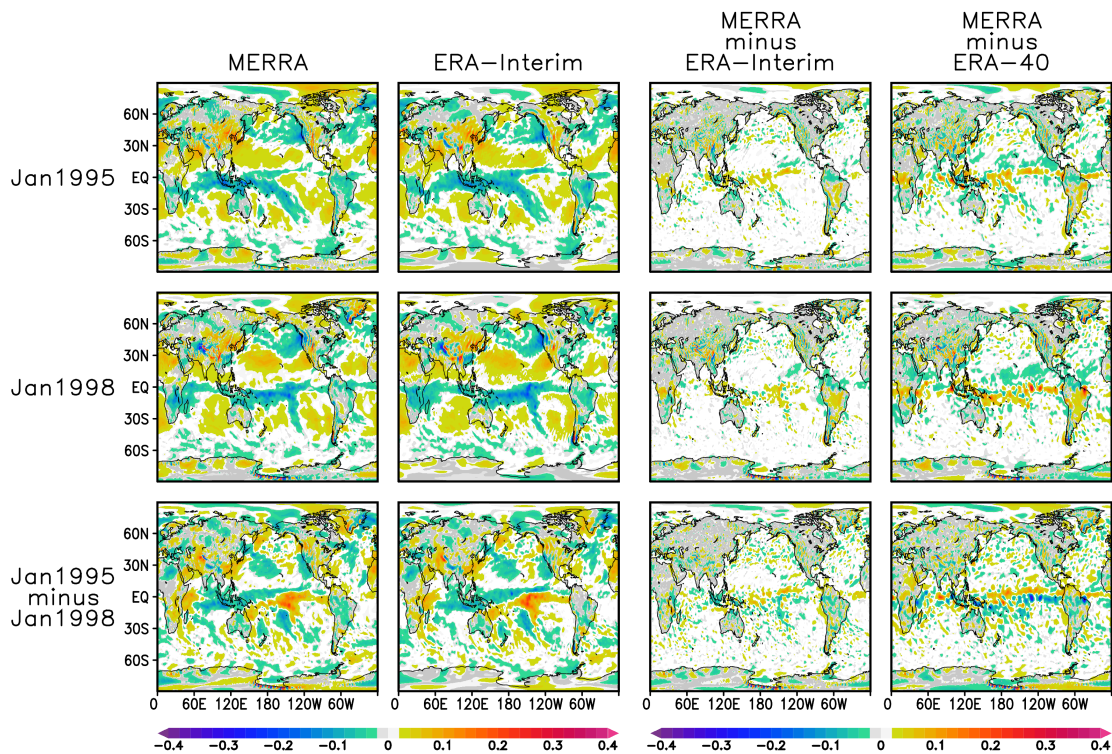


Figure 14: The vertical velocity (Pa s^{-1}) at 500 hPa for January 1995 (upper row) and January 1998 (middle row) from MERRA (first column) and ERA-Interim (second column). The differences between MERRA and ERA-Interim are shown in the third column while the fourth column compares MERRA with ERA-40. The bottom panels show the differences between the two years.

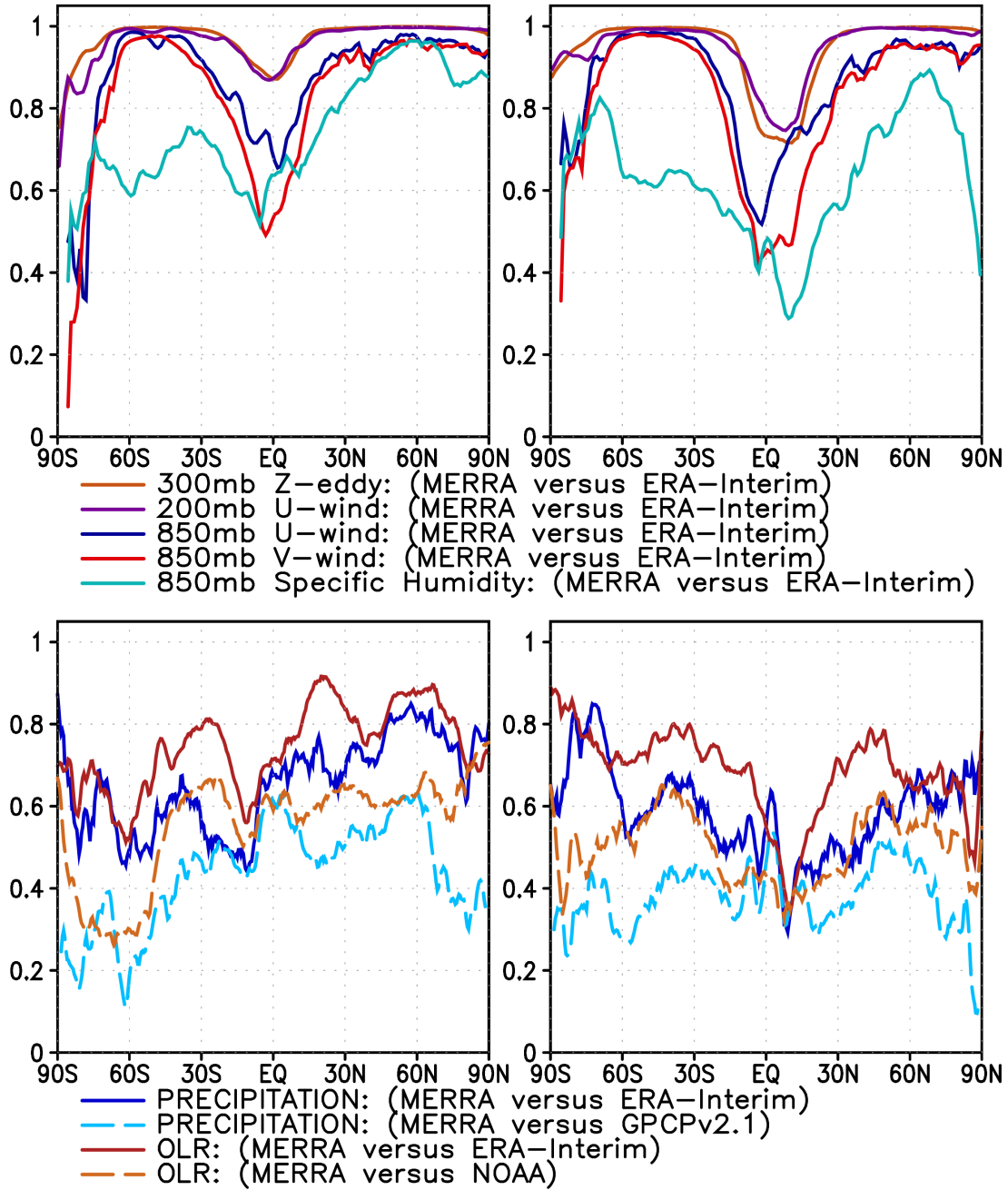


Figure 15: Zonal mean values of the correlation between MERRA and ERA-Interim, and between MERRA and selected observation data sets, for various monthly-mean quantities during January (left-hand panels) and July (right-hand panels) for the period 1990 to 2008. Comparisons with GPCP precipitation and from NOAA’s OLR product are also included.

Figure 15 shows the zonal mean values of the interannual correlations between monthly-mean quantities from MERRA and ERA-Interim, and between MERRA and selected observational data sets, for various quantities during January and July. While the correlations are generally high for dynamical variables such as tropospheric winds and eddy height (top panel), they are considerably lower for thermodynamic and cloud-related variables such as precipitation and outgoing long-wave radiation (OLR) (lower

panel). The most challenging region for all quantities is obviously the tropics, more so for the near-surface winds than for the upper tropospheric winds. The higher correlations between MERRA and ERA-Interim for precipitation and OLR, compared with the correlations between MERRA and the Global Precipitation Climatology Project (GPCP, Adler et al. 2003) or MERRA and the NOAA OLR product, emphasize the fact that the reanalyses are still more like each other than they are like the observational estimates.

7. Precipitation Estimates

Bosilovich et al. (2011, hereafter B2011) examined the energy and water budgets in MERRA, and compared cloud and precipitation estimates from the latest reanalyses with available observations. They used the precipitation from GPCP as the standard, but included the product from the Climate Prediction Center (CPC) Merged Analysis of Precipitation (CMAP, e.g., Xie and Arkin 1996) as a comparison to give some indication of the uncertainty in the observational products. The spatial correlation of the annual-mean precipitation from the analyses with the GPCP estimates (Figure 16a) shows that the three new reanalyses are closer to the observations than previous products and are approaching the correlation between the two observational estimates. In addition to these improvements in the spatial distribution of precipitation, MERRA and ERA-Interim also show a marked decrease in its spatial variance (Figure 16b), bringing them within the variance of the observational products. CFSR is somewhat higher, particularly in recent years. Note the variance from the NCEP/NCAR reanalysis (R1) is also close to the observed, but with a poor spatial structure (Figure 16a). In B2011, the improved agreement of the new reanalyses with the observed products is attributed to improvements over ocean regions, especially the tropical oceans.

It is important to point out that none of these reanalyses generates a precipitation analysis, i.e., precipitation is not a control variable in the analysis procedure. Although microwave-retrieved rain-rate observations are assimilated in the GSI over ocean areas, these data are given a low weight and have only a weak impact on increments in temperature, specific humidity, and other control variables (Treadon et al. 2002). In sensitivity and tuning experiments conducted prior to MERRA production, the three-dimensional humidity observations (moisture-sensitive radiance data from the Special Sensor Microwave Imager (SSM/I) and AMSU-B) were found to have a much larger impact on the precipitation than the precipitation observations themselves. Since the precipitation itself is not a control variable, in MERRA the precipitation product is stored from the “corrector” segment of the IAU cycle (see Figure 1). The concatenation of these segments results in a single model run in which an extra tendency term, which changes at the end of each analysis cycle and accounts for the analysis increment, is added to each control variable. In this way, only the tendency of the state can have discontinuities and not the state itself. This significantly lowers the shock in precipitation that is experienced by systems that increment the state at the beginning of each analysis cycle. Ameliorating this shock is particularly important in 3D-VAR systems such as GSI.

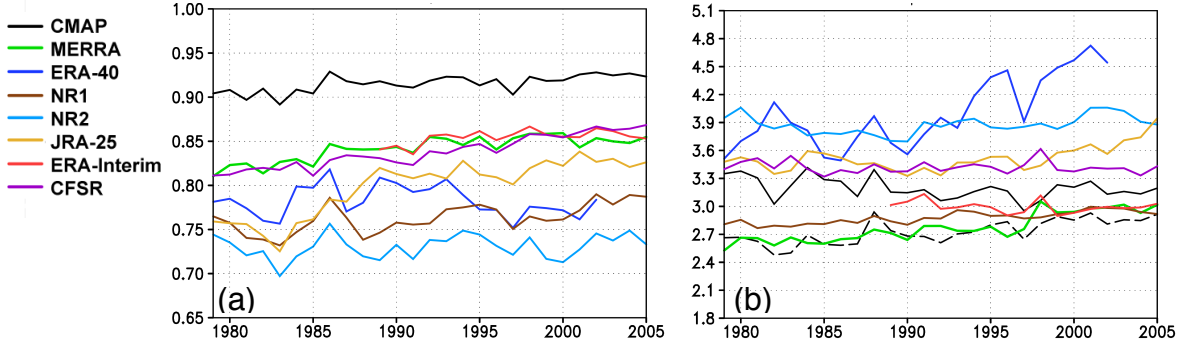


Figure 16: (a) The time series of the spatial correlation of annual mean precipitation averaged over the tropics (15°S-15°N, left hand figure) from several reanalyses with that from GPCP. The comparison of CMAP against GPCP is also shown (black curve). (b) The annual mean spatial standard deviation of precipitation (mm day^{-1}) over the tropics. The black dashed line denotes GPCP.

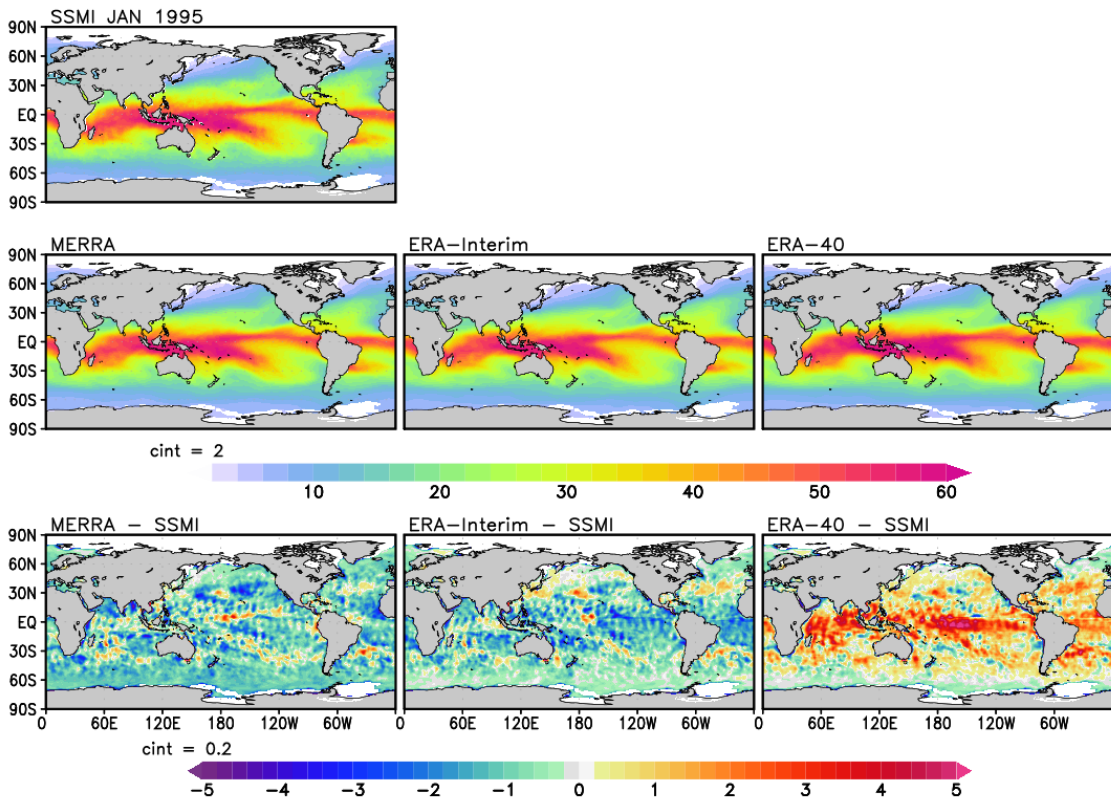


Figure 17: Monthly-mean total column water vapor (kg m^{-2}) for January 1995. The upper row is the observed field from the SSM/I product of Ferraro et al. (1996). The middle row shows MERRA (left-hand), ERA-Interim (center) and ERA-40 (right-hand). The bottom row is the difference of the reanalyses from the SSM/I data.

The precipitation distribution is obviously related to the precipitable water in the atmosphere. Figure 17 shows that MERRA and ERA-Interim display similar biases in the

total column water vapor (TCWV) relative to the gridded SSM/I product of Ferraro et al. (1996). The bias patterns are very similar although MERRA has a larger negative bias in the southern high latitudes while ERA-Interim has a larger negative bias near the equator. The biases are lower than those in ERA-40 and are of opposite sign in the tropics. Interestingly, regions of positive bias in the mid-latitudes are consistent across all three reanalyses (at least for this particular month). For comparison, Alishouse et al. (1990) used collocated radiosondes to estimate the RMS accuracy of SSM/I-derived TCWV over the ocean as approximately 2.4 kg/m^2 . They estimated the bias in the tropics to be about the same level $[(-2.1, 0.5, 2.4) \text{ kg/m}^2]$ in the respective bands ($20^\circ\text{S}-0^\circ$, $0^\circ-20^\circ\text{N}$, $20^\circ-25^\circ\text{N}$), and the bias in the higher latitudes to be less than 1 kg/m^2 $[(0.6, -0.9, 0.8) \text{ kg/m}^2]$ in the respective bands ($55^\circ-25^\circ\text{S}$, $25^\circ-55^\circ\text{N}$, $55^\circ-60^\circ\text{N}$).

a. Impact of observing system changes on precipitation estimates

The time series of global monthly-mean precipitation (Figure 18) provides perhaps the clearest evidence that, despite the major advances, the latest reanalyses are still significantly impacted by changes in the observing system. There is a trend (or series of jumps and different trends) in MERRA associated with the introduction of SSM/I observations in July 1987 and of AMSU-A data from NOAA-15 in November 1998. There is a clear indication (from experiments in which particular instruments or channels were withheld from the assimilation, also shown in Figure 18) that the global precipitation in MERRA is sensitive to AMSU-A data, and in particular to the window channels, 1-3 and 15 (see Robertson et al. 2011 and the inset of Figure 18). In contrast, ERA-Interim, which does not assimilate those window channels, is sensitive to the assimilation of SSM/I data (Dick Dee 2010, personal communication).

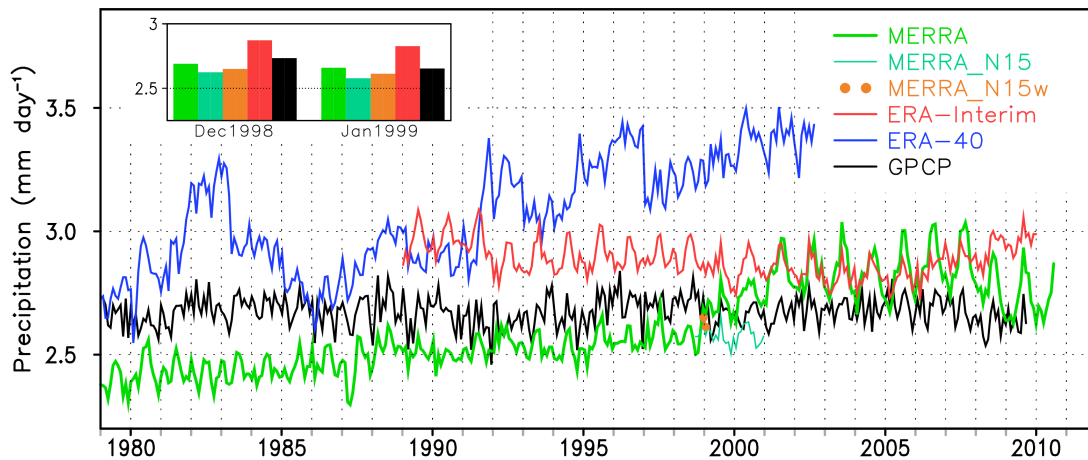


Figure 18: Time series of global monthly mean precipitation (mm day^{-1}) for MERRA, ERA-Interim and ERA-40, compared against GPCP. In addition to the time series from the MERRA distribution, two short data withholding experiments are shown. MERRA_N15 is from an experiment withholding all AMSU-A data from NOAA-15, and MERRA_N15w withhold only the AMSU-A window channels, 1-3 and 15. For clarity, the inset shows the monthly mean values for December 1998 and January 1999.

The dates of changes in the availability of AMSU-A and SSM/I data, and in the rain-rate data from the TRMM Microwave Imager (TMI), are presented in Table 1. Matching

these dates with notable changes in Figure 18, it appears that MERRA responds more to AMSU-A than to SSM/I. Significant increases in precipitation are observed with the introduction of AMSU-A on NOAA-15 in 1998 and NOAA-16 in 2001, although there is little discernible impact from the introduction of a third AMSU-A on NOAA-18 in 2005. The loss of AMSU-A on NOAA-16 in 2008 coincides with a clear decrease in global mean precipitation, although further investigation is required to determine whether the loss of SSM/I on F14 around this time also contributes to the decrease.

The sensitivity of precipitation to changes in the observing system are investigated further in Figure 19, which shows the evolution of the zonal-mean, monthly-mean interannual anomalies of MERRA precipitation, together with the vertically integrated moisture increment from the analysis. Robertson et al. (2011) discusses these time series in detail. Except for the marked interannual variability in precipitation in the tropics associated with ENSO, there is close agreement between variations in the moisture increment and precipitation south of about 30°N. There is less similarity in the Northern Hemisphere where, presumably, the conventional data help to ameliorate changes associated with the satellite observations. Comparing Figure 19 with Table 1 indicates that MERRA is sensitive to the SSM/I data. However, whereas SSM/I data tend to dry the atmosphere, AMSU-A data appear to have an overwhelming moistening effect almost everywhere.

Table 1. Dates of observing system changes that appear to impact the global mean precipitation as seen in Figure 18.

Date of Data Change	Data Change
1987/7	SSM/I F08 introduced
1990/12	SSM/I F10 introduced
1991/12/04	SSM/I F08 not available
1991/12	SSM/I F11 introduced
1995/5	SSM/I F13 introduced
1997/5	SSM/I F14 introduced
1997/11/13	SSM/I F10 not available
1997/12	TMI rain rate introduced
1998/11	N-15 AMSU-A introduced
1999/12	SSM/I F15 introduced
1999/12/17	SSM/I F11 not available
2001/1/1	N-16 AMSU-A introduced
2002/10	EOS/Aqua AMSU-A introduced
2005/11/1	N-18 AMSU-A introduced
2006/07/25	SSM/I F15 not available
2008/3/4	N-16 AMSU-A not available
2008/08/23	SSM/I F14 not available
2009/11/18	SSM/I F13 not available

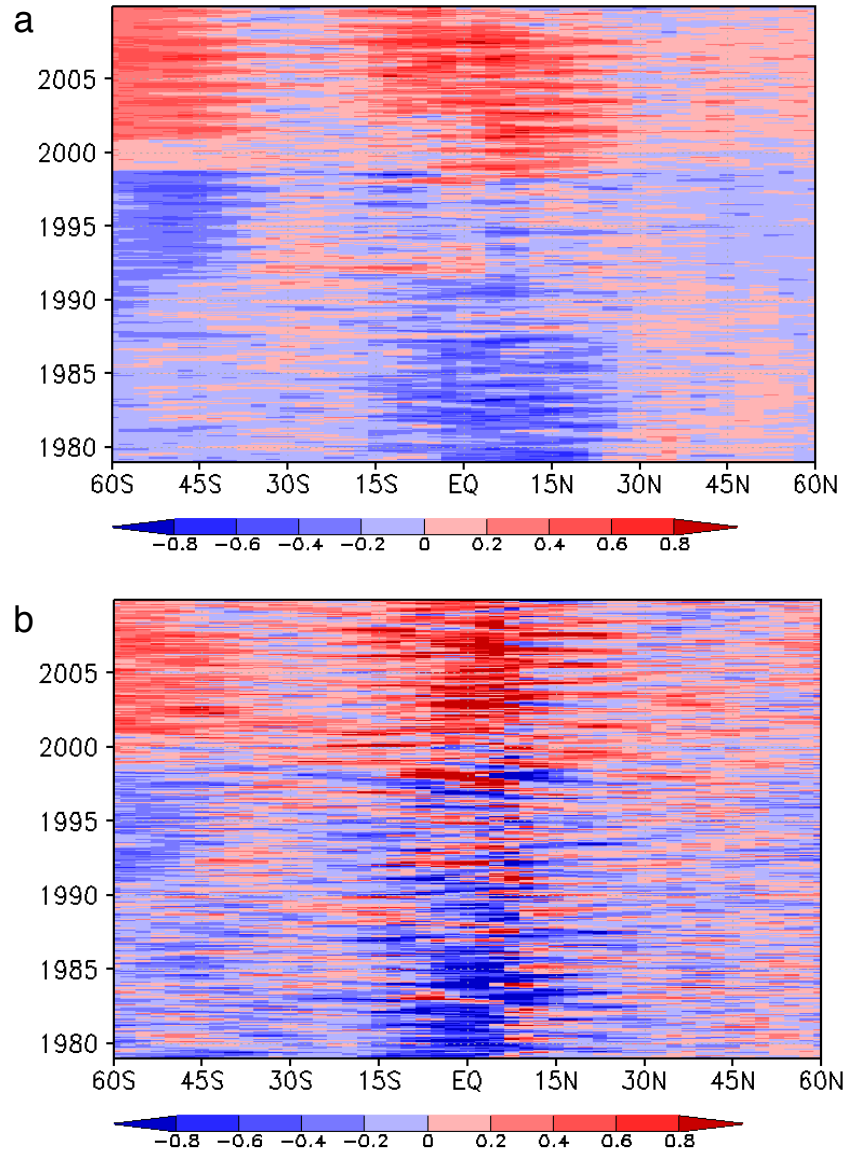


Figure 19: Zonal mean values of interannual anomalies of (a) vertically integrated moisture increments and (b) precipitation. Units for both quantities are mm day^{-1} . Anomalies are departures from climatological mean seasonal cycles (see Robertson et al. 2011).

Despite these issues, the fact that the global-mean and all measures of the spatial distribution of precipitation in both MERRA and ERA-Interim are closer to the GPCP estimates than those of other reanalyses reflects the progress that has been made in representing the hydrologic cycle. However, given the given the relative magnitude of the analysis increment in the atmospheric water budget (discussed below) and of the remaining sensitivities to the observing system, we must conclude that even these reanalyses are not yet providing new information, beyond what is available in the CMAP and GPCP products, and that they are particularly unsuitable to the study of trends.

b. Analysis contributions to the water budget

One of the important contributions from MERRA to water and energy budget studies is the careful attention paid to tracking all terms needed to close the budgets. All such terms are calculated inline during the assimilation cycle so as to produce an exactly closed budget. The terms include contributions from the analysis increments, and even (for example) the small “spurious” snow-related energy sources and sinks associated with several small accounting inconsistencies across the coupled land and atmospheric models. The budget terms are presented in the MERRA file specification document as well as in B2011.

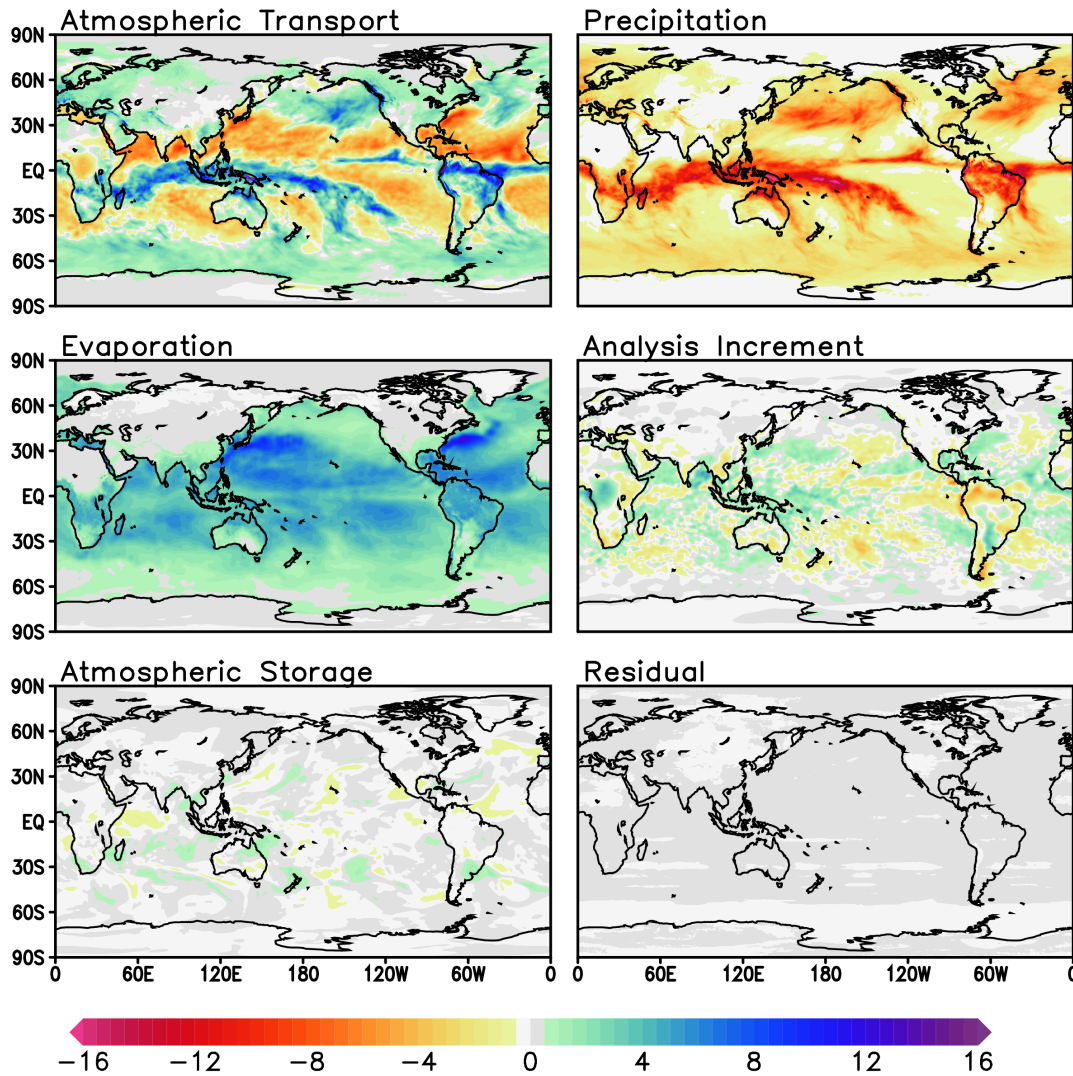


Figure 20: MERRA’s estimate of the vertically integrated water vapor budget for January 2004, in $\text{kg m}^{-2} \text{day}^{-1}$.

The size of the analysis increments is one measure of the quality of the system, especially in terms of bias. Ideally, the increments should be small and nonsystematic. Figure 20 shows the vertically integrated water vapor budget for January 2004. Clearly, the analysis increment is much smaller in amplitude and has smaller scale variability than the

dominant terms in the budget – the atmospheric transport, precipitation, and evaporation. However, since the analysis increment is larger than the storage term (the total change in integrated water vapor over the month), it does make a non-trivial contribution to the overall budget.

c. Precipitation impacts on land surface hydrology in MERRA

Precipitation is the most important driver of land surface hydrological conditions, with an overwhelming impact on the accuracy of simulated hydrological fields. Although the climatological distribution of MERRA precipitation is quite good, remaining biases in the long-term climatology and higher frequency errors, particularly in the diurnal cycle, have a severe impact on the soil wetness estimates, as pointed out by Reichle et al. (2011). They note three deficiencies in particular: (i) MERRA precipitation rates are less intense than observed and tend to appear as persistent drizzle; (ii) MERRA precipitation tends to be highest in the middle of the day, whereas the observations show frequent nighttime rain maxima; and (iii) MERRA incoming solar radiation during daytime precipitation events is not reduced as much as in observations. Taken together, these three deficiencies lead to immediate re-evaporation of much of the rainfall from droplets sitting on the surface of the vegetation canopy, which implies that not enough of the water is allowed to fall through the canopy and ultimately infiltrate the soil or contribute to surface runoff.

Reichle et al. (2011) undertakes offline (land-only) "MERRA-Land" simulations with two key changes: (i) the MERRA precipitation forcing is corrected by the pentad data from GPCP, and (ii) some parameters of the Catchment model are modified to compensate for the precipitation deficiencies. Comparisons are then made with *in situ* observations and independent global data products to evaluate the land surface hydrology from MERRA and MERRA-Land estimates. The revised model parameters considerably improve the average interception loss ratio and contribute to more realistic latent heat fluxes in MERRA-Land. Generally, the skill of MERRA and MERRA-Land estimates of soil moisture and runoff is comparable to that of ERA-Interim estimates. Moreover, snow depth and snow water equivalent compare well against *in situ* observations and the snow analysis from the Canadian Meteorological Center. Average anomaly correlation (R) skill levels for MERRA and MERRA-Land surface hydrological variables generally range from $R \sim 0.5$ to $R \sim 0.8$, with MERRA-Land skills being slightly higher (with statistical significance) than MERRA skills.

8. The stratosphere

As noted earlier, in addition to other applications, meteorological analyses produced by the GEOS DAS provide wind fields for transport studies by the stratospheric chemistry community. Hence the quality of the analysis in the stratosphere is an important performance metric. In the Arctic lower stratosphere, the dominant components of the climate and variability were well represented in early analyses produced with low model tops (e.g., Pawson and Fiorino 1998a) since the large-scale structure in this region is well sampled by radiosondes. Even in the Antarctic, temperature retrievals from space-based data were adequate to constrain the polar vortex structure, but early analyses did not capture low temperatures characteristic of the polar regions. Increasing the height of the upper boundary led to substantial improvements in the analyzed structure of the middle

stratosphere in ERA-40, ERA-Interim and MERRA compared to the earlier products (Pawson et al. 2011). These model improvements coupled with improved use of space-based radiance observations have led to consistent and accurate analyses of the middle and polar latitudes in both hemispheres, up to altitudes of 30-40 km. At higher levels, even the most recent analyses are less successful. Manney et al. (2008a, b) demonstrated that structures in the upper stratosphere and mesosphere are not well captured in analyses performed using systems that assimilate only nadir-sounding radiance observations, the dominant data type in the reanalyses.

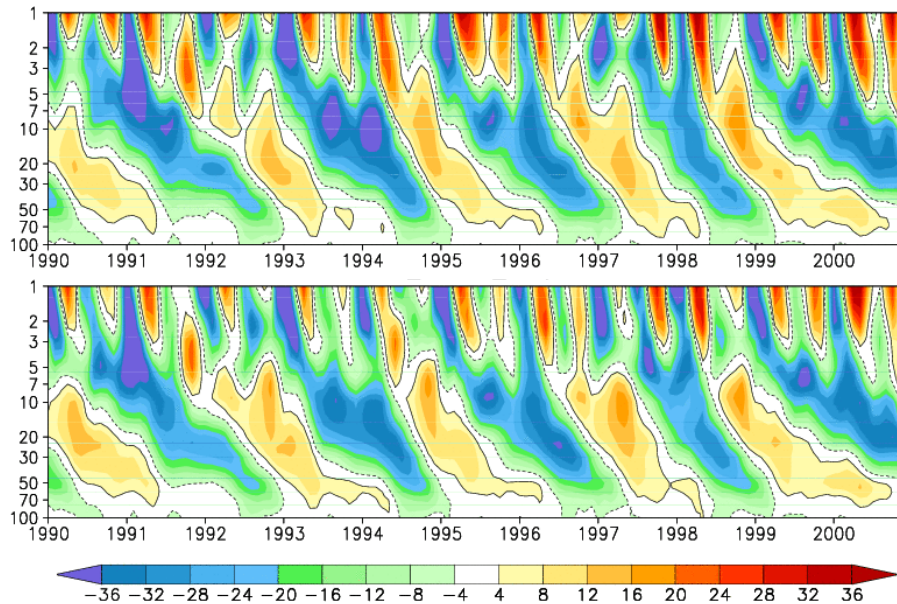


Figure 21: Time series of the QBO and SAO as seen from the zonal-mean zonal wind component averaged between 10°S and 10°N in MERRA (upper) and ERA-Interim (lower).

In the tropics, the quasi-biennial oscillation (QBO) evident in the zonal-mean wind field has not always been captured well in reanalyses. It was reasonably well represented by ERA-15 but not by NCEP/NCAR R1 (Pawson and Fiorino 1998b) or the earlier GEOS analyses. Reasons for this are not entirely clear, although Gaspari et al. (2006) showed that adequately long length scales are needed to spread wind information from sparse radiosondes around the globe, and that inadequate data selection can readily lead to good observations being rejected in favor of poor analyses in the tropical stratosphere. ERA-40 improved upon the representation in ERA-15 (Baldwin and Gray, 2005) and now ERA-Interim analyses of the QBO are in excellent agreement with observations. Figure 21 shows that MERRA too has realistic zonal wind variability in the lower stratosphere.

Zonal-mean winds in the tropical upper stratosphere are dominated by the semi-annual oscillations (SAO), with transitions between easterly and westerly phases concentrated in shallow layers with large vertical shears (say $10 \text{ ms}^{-1}/\text{km}$), which are associated with meridional curvature in the temperature field. The weak temperature gradients and the

vertical averaging caused by the thick weighting functions associated with nadir radiance observations, as well as the lack of accurate balance constraints between winds and temperature fields in the tropics, mean that there is little observational constraint on the SAO winds in the reanalyses. It is thus not surprising that there are differences between the tropical upper stratospheric winds from different reanalysis products (Figure 21).

9. MERRA Products and Access

a. Products

A complete list of the analyzed and diagnosed fields produced by MERRA is given in the product file specification document available at the GMAO's MERRA website <http://gmao.gsfc.nasa.gov/merra/>. A small advisory group helped to define the comprehensive set of enhanced post-processed products that would be useful for supporting water and energy budget studies as well as chemical-transport modeling. The use of the IAU allows for higher frequency products during the corrector segments depicted in Figure 1 (“assimilation products”) in addition to the traditional six-hourly products that are produced directly from the analysis (“analyzed products”).

Table 2. A summary of the MERRA product collections and their characteristics.

<i>Collection Type</i>	<i>Number of Collections</i>	<i>Characteristics</i>	<i>Frequency</i>
<i>Invariants</i>	2		
<i>Analyzed Fields</i> <i>[u, v, t, q, O₃, p]</i>	2	Native grid, instantaneous fields Model and Pressure level collections	6-hourly
<i>Assimilated Fields</i>	1	Reduced grid, instantaneous fields Pressure levels	3-hourly
<i>3-D Diagnostics</i>	8	Reduced grid, time-averaged fields Pressure levels	3-hourly
<i>2-D Diagnostics</i>	4	Native grid, time-averaged fields	Hourly
	1	Native grid, time-averaged land-related surface fields	Hourly
	1	Native grid, time-averaged ocean-related surface fields	Hourly
	1	Native grid, instantaneous vertical integrals	Hourly
<i>Fields for offline Chemistry Transport Models</i>	6	Various resolutions, grids, frequencies	

There are two time-invariant and 24 time-varying product collections; some are on the model's native horizontal grid, $1/2^\circ \times 2/3^\circ$, and some are at reduced resolution, either $1^\circ \times 1.25^\circ$ or $1.25^\circ \times 1.25^\circ$. A brief summary of products is provided in Table 2. Detailed information and a description of each variable are available in the MERRA file specification document. As mentioned earlier, MERRA provides closed atmospheric budgets, including the analysis increment terms. The observational forcing from the assimilation increments during the corrector segments is tallied in the output budgets of the model (e.g. water and enthalpy). Bosilovich et al. (2011) provides examples of the magnitudes of these terms in water and energy budgets.

b. Accessing MERRA data and information

The MERRA products are available online through the Goddard Earth Sciences Data and Information Services Center (GES DISC), see <http://disc.sci.gsfc.nasa.gov/daac-bin/DataHoldings.pl>. Several different access options are available, including OPeNDAP and FTP. An FTP subsetter facilitates downloads of partial data sets. Online visualization options using the Giovanni web-based application developed by the GES DISC (Acker and Leptoukh, 2007) are also available. An online atlas of climatological information from MERRA, including comparisons with data-only products and other reanalyses, is being maintained at <http://gmao.gsfc.nasa.gov/ref/merra/atlas/>.

10. Summary and Issues for the Next Generation of Reanalyses

In most aspects, MERRA has achieved its primary goals of improving significantly on the previous generation of reanalyses in the representation of the atmospheric branch of the hydrological cycle and in providing complete information for budget studies. The availability of other updated reanalyses from ECMWF (ERA-Interim, 1988 to the present) and NCEP (CFSR, 1979 to the present) have provided a useful basis for evaluating MERRA and identifying common deficiencies that need to be addressed in the next generation of reanalyses.

Users of reanalysis data often request a characterization of the quality of and the uncertainty in the fields. While intercomparison with reference data sets is common practice for ascertaining quality, such comparisons are usually restricted to long-term climatological statistics and seldom provide state-dependent measures of the uncertainties involved. A new look at the information available during the assimilation process, such as the gridded innovations and contextual bias presented in Da Silva (2011), provide additional information on the quality of the analyses, as well as on how different observations are represented in the analysis. In addition to sharing observations, it would be useful for reanalysis producers to share such information on system performance in order to guide future development. The sharing of these and other metrics as part of future reanalyses would benefit users as well.

As suggested in Sections 6, 7, and 8, as model biases are reduced so that assimilation increments are smaller, the differences in the climate variability from different reanalyses are also reduced. However, there are still substantial differences between the existing reanalyses in poorly constrained quantities such as precipitation and surface fluxes due to

differences in the assimilating models and in how the models interact with the assimilated data. These differences are an important measure of the uncertainty in reanalysis products. Observing system changes, which often manifest themselves in reanalysis time series by abrupt variations or discontinuities, can exacerbate such differences. These impacts from observing system changes must be distinguished from real climate variations and pose perhaps the greatest challenge for the next generation of reanalyses.

The performance of the reanalyses in the high stratosphere is also a cause for concern. A major issue is the lack of long-term *in situ* temperature observations, which, coupled with the model biases and the deep weighting functions of the SSU and AMSU-A radiance channels, makes it difficult to place precise constraints on the meteorological fields at these levels. It also makes the application of the variational bias correction of the observations inappropriate because of the major influence of model bias in the absence of other “anchoring” data. Future reanalyses will need to focus on improving models and better calibration of the input radiance data. Limb-sounding temperature data are available for certain periods, and may be used as anchors for a limited number of years, but these datasets generally do not overlap, so issues related to cross-dataset bias have not been addressed in detail. High-quality temperature time series are available from occultation measurements, but the extremely low density of these data makes them unsuitable for assimilation. A more promising way of using them in reanalyses may be as calibration datasets – an aspect that will require substantial developments.

In spite of these challenges, significant improvements have come from each generation of reanalyses. Both the improvements and many of the remaining deficiencies are apparent in the time series of global-mean precipitation. Most of the improvements have come from the numerical weather prediction imperative, for which the assimilation systems will continue to evolve, taking advantage of new data types and improved methodologies. However, the question remains as to what might be done to improve reanalyses specifically, especially to address jumps and trends associated with changes in the observing system.

Thorne and Vose (2010) make some suggestions for how to undertake a climate reanalysis that will support trend analysis. Some of those suggestions – thinning the data to reduce shocks to the system, assimilating only long-term satellite observations, assimilating only raw data (not bias-corrected or cross-calibrated data) – run counter to the experience of reanalysis developers to date (Dee et al. 2010). For example, the different biases in MSU instruments from one satellite to the next (Zou et al. 2006) or in IR instruments (DU09) mean that there are no long-term *homogeneous* satellite observations, even from TOVS. Without careful bias correction, derived fields like precipitation are not adequate for climate variability studies, much less climate trend analysis. Nevertheless, for some applications, the reanalysis community needs to continue to seek ways to generate a climate analysis that minimizes the impact of changes in the observing system while preserving the wealth of information gained as better observation are added. A workshop on improving observations for reanalysis (Schubert et al. 2006) recommended improvements to historical observations (including data mining), improved quality control, and further cross-calibration and bias-correction of observations to help to reduce the impacts from changes in the observing system.

Continued interactions and collaborations between the producers of reanalyses, as well as with the data stewards, will be needed to make progress on these issues (Rienecker et al. 2011). In the meantime, the availability of three new reanalyses—MERRA, CFSR and ERA-Interim—plus the anticipated availability of a new Japanese 55-yr Reanalysis (JRA-55) provide researchers with a *de facto* ensemble of state-of-the-art climate analyses for making robust quality assessments and quantifying uncertainties.

Acknowledgements

The GEOS-5 AGCM and DAS development and the MERRA project in the Global Modeling and Assimilation Office was funded by NASA's Modeling, Analysis and Prediction program. That support is gratefully acknowledged. We thank Derek van Pelt for providing some of the figures for this paper, for assembling the online atlas and contributing to monitoring MERRA through the production phases. We thank the many others in the GMAO who contributed in various ways to the production and monitoring of MERRA. Dana Ostrenga, of the GES DISC, worked tirelessly with us to have MERRA distributed online. We gratefully acknowledge her contributions with those of her colleagues in the GES DISC. We thank Leopold Haimberger of the University of Vienna for generating new corrections with RAOBCORE V1.4 with the corrected Vaisala RS-80 sondes. Laurie Rokke contributed to the development of the radiative transfer module used for SSU. SSM/I data produced by Remote Sensing Systems was sponsored by the NASA Earth Science MEaSUREs DISCOVER Project. Data are available at www.remss.com. Support from the NASA Center for Climate Simulation (NCCS), providing a production environment for timely delivery of MERRA, was essential to the project. Finally, and not least, we thank the MERRA User Group who provided invaluable advice during the testing phase of MERRA, helped identify the product suites needed for a broad community of users, and then gave the final approval for production. The User Group was Phil Arkin (chair, University of Maryland), Alan Betts (Atmospheric Research), Robert Black (Georgia Institute of Technology), David Bromwich (Ohio State University), John Roads (Scripps Institution of Oceanography), Jose Rodriguez (Goddard Space Flight Center), Steve Running (University of Montana), Paul Stackhouse, Jr. (Langley Research Center), Kevin Trenberth (National Center for Atmospheric Research), and Glenn White (NOAA/NCEP).

Appendix A. Observations used in MERRA production

Table A.1 Conventional data in MERRA, availability and data sources.

DATA SOURCE/TYPE	PERIOD	DATA SUPPLIER
RAOBS/PIBALS/DROPS	1970 – present	See Table A.2
Wind profiles	1992/5/14 - present	NCEP CDAS
Conventional, ASDAR, and MDCRS aircraft reports	1970 – present	NOAA/NCEP, ECMWF
PAOB	1978 – 2010/8/17	NCEP, ECMWF, JMA, BOM
GMS, METEOSAT, IR and visible winds	1977 – present	NOAA/NCEP, JMA
GOES cloud drift winds	1978 – present	NOAA/NCEP
EOS/Terra/MODIS winds	2002/7/01 - present	NOAA/NCEP
EOS/Aqua/MODIS winds	2003/9/01 - present	NOAA/NCEP
Surface land observations	1970 - present	NOAA/NCEP
Surface ship and buoy observations	1970 - present	ICOADS
SSM/I rain rate, GPROF algorithm (Kummerow et al., 2001)	1987/7 - present	NASA/GES DISC
SSM/I V6 wind speed (Wentz, 1997)	1987/7 - present	Remote Sensing Systems (RSS)
TMI rain rate	1997/12 - present	NASA/GES DISC
QuikSCAT surface winds	1999/7 - present	Jet Propulsion Laboratory
ERS-1 surface winds	1991/8/5 – 1996/5/21	CERSAT
ERS-2 surface winds	1996/3/19 – 2001/1/17	CERSAT
SBUV2 ozone (Version 8 retrievals)	1978/10 - present	NASA/GES DISC

Table A.2 Historical radiosonde, dropsonde, and PIBAL archive sources.

NCEP/NCAR	OfficeNote20, OfficeNote29, NMC/NCEP/GTS ingest
ECMWF	ECMWF/FGGE, ECMWF/MARS/GTS ingest
JMA	Japan Meteorological Agency GTS ingest
NCAR	International archives: Argentina, Australia, Brazil, Canada, China, Dominic, France, India, Japan, NCDC, New Zealand, Russia, Singapore, South Africa, UK Research sets: PermShips, RemoteSites, Ptarmigan, Scherhaug, LIE, GATE, BAS
NCDC	US military and academic sources: TD52, TD53, TD54, TD90, USCNTRL, USAF, NAVY, CCARDS, MIT

Table A.3 Satellite radiance data in MERRA, availability and data sources.

DATA SOURCE/TYPE	PERIOD	DATA SUPPLIER
TOVS/tn (TIROS N)	1978/10/30 – 1980/06/01	NCAR
TOVS/na (NOAA 6)	1979/07/02 – 1983/04/17	NCAR
TOVS/nc (NOAA 7)	1981/07/11 - 1986/06/01	NCAR
TOVS/ne (NOAA 8)	1983/04/26 - 1985/01/01	NCAR
TOVS/nf (NOAA 9)	1985/01/01 - 1988/11/01	NOAA/NESDIS & NCAR
TOVS/ng (NOAA 10)	1986/11/25 - 1991/09/17	NOAA/NESDIS & NCAR
TOVS/nh (NOAA 11)	1988/09/02 - 1994/12/31	NOAA/NESDIS & NCAR
TOVS/nd (NOAA 12)	1991/08/18 - 1997/07/14	NOAA/NESDIS & NCAR
TOVS/nj (NOAA 14)	1995/01/19 - present	NOAA/NESDIS
TOVS/nk (NOAA 15)	1998/07/01 - present	NOAA/NESDIS
TOVS/nl (NOAA 16)	2001/03/02 - present	NOAA/NESDIS
TOVS/nm (NOAA 17)	2003/03/01 - present	NOAA/NESDIS
TOVS/nn (NOAA 18)	2005/10/05 – present	NOAA/NESDIS
EOS/Aqua	2002/10 - present	NOAA/NESDIS
SSM/I V6 (F08)	1987/7 - 1991/12/04	RSS
SSM/I V6 (F10)	1990/12 – 1997/11/13	RSS
SSM/I V6 (F11)	1991/12 – 1999/12/17	RSS
SSM/I V6 (F13)	1995/5 – 2009/11/18	RSS
SSM/I V6 (F14)	1997/5 – 2008/08/23	RSS
SSM/I V6 (F15)	1999/12 – 2006/07/25	RSS
GOES sounder T _B	2001/01 – 2007/12/3	NOAA/NCEP
SBUV2 ozone (Version 8 retrievals)	1978/10 - present	NASA/GSFC/DAAC

Appendix B. Acronyms

3D-Var	Three-dimensional Variational assimilation
A-F	Analysis Minus Background (or First guess)
AGCM	Atmospheric General Circulation Model
AIREP	AIRcraft REPort
AIRS	Advanced Infrared Sounder (on Aqua)
AMI	Active Microwave Instrument
AMSU	Advanced Microwave Sounding Unit (on later TIROS)
AQUA	EOS PM satellite
ASDAR	Aircraft to Satellite DATA Relay system
ATOVS	Advanced TIROS Operational Vertical Sounder
AURA	EOS CHEM satellite
BOM	Australian Bureau of Meteorology
BUFR	Binary Universal Form for the Representation of meteorological data
CCARDS	Comprehensive Aerological Reference Data Set, Core Subset
CDAS	Climate Data Assimilation System
CERSAT	Center for Satellite Exploitation and Research
CFSR	Climate Forecasting System Reanalysis
CMAP	Climate Prediction Center (CPC) Merged Analysis of Precipitation
CRTM	Community Radiative Transfer Model
DAS	Data Assimilation System
ECMWF	European Centre for Medium Range Weather Forecasting
ENSO	El Niño-Southern Oscillation
EOS	Earth Observing System
ERA	ECMWF Re-Analysis
ERS-1, 2	Environmental Research Satellite (surface winds from AMI)
ESMF	Earth System Modeling Framework
FGGE	First GARP Global Experiment
FTP	File Transfer Protocol
GARP	Global Atmospheric Research Program
GATE	GARP Atlantic Tropical Experiment
GEOS	Goddard Earth Observing System
GES DISC	Goddard Earth Sciences Data and Information Services Center
GMAO	Global Modeling and Assimilation Office (GSFC)
GMS	Geostationary Meteorological Satellite
GOCART	Goddard Chemistry, Aerosol, Radiation, and Transport
GOES	Geosynchronous Operational Environmental Satellite
GPCP	Global Precipitation Climatology Project
GPROF	Goddard Profiling algorithm
GSFC	(NASA) Goddard Space Flight Center
GSI	Grid-point Statistical Interpolation
GTS	Global Telecommunication System
HALOE	Halogen Occultation Experiment
HIRS	High resolution Infrared Radiation Sounder
IAU	Incremental Analysis Update
ICOADS	International Comprehensive Ocean-Atmosphere Data Set

IR	Infrared
JMA	Japan Meteorological Agency
JRA	Japanese Reanalysis
MARS	ECMWF's Meteorological Archive and Retrieval System
MDCRS	Meteorological Data Collection and Reporting System
MERRA	Modern-Era Retrospective analysis for Research and Applications
MIT	Massachusetts Institute of Technology
MLS	Microwave Limb Sounder
MODIS	Moderate Resolution Imaging Spectroradiometer
MSU	Microwave Sounding Unit
NASA	National Aeronautics and Space Administration
NCAR	National Center for Atmospheric Research
NCDC	National Climatic Data Center
NCEP	National Centers for Environmental Prediction
NESDIS	National Environmental Satellite, Data, and Information Service
NMC	National Meteorological Center
NOAA	National Oceanic and Atmospheric Administration
O-A	Observation Minus Analysis
O-F	Observation Minus Background (or First Guess)
OLR	Outgoing Long-wave Radiation
OPeNDAP	Open-source Project for a Network Data Access Protocol
PAOBS	Synthetic surface Pressure OBS
PBL	Planetary Boundary Layer
PDF	Probability Density Function
PIBAL	PILot BALloon
QBO	Quasi-Biennial Oscillation
QC	Quality Control
QuikSCAT	Quick Scatterometer
R1	NCEP/NCAR Reanalysis
RAOB	Radiosonde Observations
RAOBCORE	Radiosonde Observation Bias Correction Using Reanalyses
RMS	Root Mean Square
RSS	Remote Sensing Systems
SAO	Semiannual Oscillations
SBUV/2	Solar Backscatter Ultraviolet Spectral Radiometer-2
SNO	Simultaneous Nadir Overpass
SSM/I	Special Sensor Microwave/Imager
SSU	Stratospheric Sounding Unit
TCWV	Total Column Water Vapor
TERRA	EOS AM Satellite
TIROS	Television and Infrared Observatory Spacecraft
TMI	TRMM Microwave Imager
TOVS	TIROS Operational Vertical Sounder
TRMM	Tropical Rainfall Measurement Mission
USAF	U.S. Air Force
USCNTRL	U.S. controlled ocean weather stations

UTC
VBC

Coordinated Universal Time
Variational Bias Correction

References

- Acker, J. G., and G. Leptoukh, 2007: Online analysis enhances use of NASA Earth Science Data, *EOS, Trans. AGU*, **88** (2), pages 14 and 17.
- Adler, R. F., and Coauthors, 2003: The version-2 global precipitation climatology project (GPCP) monthly precipitation analysis (1979-present). *J. Hydromet.*, **4**, 1147-1167.
- Alishouse, J. C., S. A. Snyder, V. Jennifer, and R. R. Ferraro, 1990: Determination of oceanic total precipitable water from the SSM/I, *IEEE Trans. Geosci. Rem. Sens.*, **28**, 811– 816.
- Bacmeister, J. T., M. J. Suarez, and F. R. Robertson, 2006: Rain re-evaporation, boundary-layer/convection interactions and Pacific rainfall patterns in an AGCM, *J. Atmos. Sci.*, **63**, 3383-3403.
- Baldwin, M. P., and L. J. Gray, 2005: Tropical stratospheric zonal winds in ECMWF ERA-40 reanalysis, rocketsonde data, and rawinsonde data. *Geophys. Res. Lett.*, **32**, L09806, doi:10.1029/2004GL022328.
- Bloom, S., L. Takacs, A. DaSilva, and D. Ledvina, 1996: Data assimilation using incremental analysis updates. *Mon. Wea. Rev.*, **124**, 1256-1271.
- Bosilovich, M. G., F. R. Robertson, and J. Chen, 2011: Energy and water budgets in MERRA. *J. Clim.* (submitted to MERRA special collection).
- Brunke, M., Z. Wang, X. Zeng, M. Bosilovich, and C.-L. Shie, 2011: An assessment of the uncertainties in ocean surface turbulent fluxes in 11 reanalysis, satellite-derived, and combined global data sets. *J. Clim.* (submitted to MERRA special collection).
- Cardinali C., L. Isaksen, and E. Anderson, 2003: Use and impact of automated aircraft data in a global 4DVAR data assimilation system. *Mon. Wea. Rev.* **131**: 1865–1877.
- Chou, M.-D. and M. J. Suarez, 1999: A Solar Radiation Parameterization for Atmospheric Studies. NASA *Technical Report Series on Global Modeling and Data Assimilation 104606*, v**15**, 40pp.
- Chou, M.-D., M. J. Suarez, X. Z. Liang, and M. M.-H. Yan, 2001: A Thermal Infrared Radiation Parameterization for Atmospheric Studies. NASA *Technical Report Series on Global Modeling and Data Assimilation 104606*, v**19**, 56pp.
- Colarco, P. R., A. da Silva, M. Chin, and T. Diehl, 2010: Global aerosol distributions in the NASA GEOS-4 model and comparisons to satellite and ground-based aerosol optical depth. *J. Geophys. Res.*, **115**, doi:10.1029/2009JD012820.
- Cullather, R. I., and M. G. Bosilovich, 2011a: The energy budget of the polar atmosphere in MERRA. *J. Clim.* (submitted to MERRA special collection).
- Cullather, R. I., and M. G. Bosilovich, 2011b: The moisture budget of the polar atmosphere in MERRA. *J. Clim.* (submitted to MERRA special collection).
- Da Silva, A. M., 2011: *J. Clim.* (submitted to MERRA special collection).
- Decker, M., M. Brunke, Z. Wang, K. Sakaguchi, X. Zeng, and M.G. Bosilovich, 2011: Evaluation of the Reanalysis Products from GSFC, NCEP, and ECMWF Using Flux Tower Observations. *J. Clim.* (submitted to MERRA special collection).

- Dee, D. P., 2005: Bias and data assimilation. *Q. J. R. Meteorol. Soc.* **131**, 3323–3343.
- Dee, D., and A. M. Da Silva, 1998: Data assimilation in the presence of forecast bias. *Q. J. R. Meteorol. Soc.*, **124**, 269–295.
- Dee, D. P., and A. da Silva, 1999: Maximum-likelihood estimation of forecast and observation error covariance parameters. Part I: Methodology. *Mon. Wea. Rev.*, **127**, 1822–1834.
- Dee, D. P., and S. Uppala, 2009: Variational bias correction of satellite radiance data in the ERA-Interim reanalysis. *Q. J. R. Meteorol. Soc.*, **135**, 1830–1841.
- Dee, D. P., E. Källén, A. J. Simmons, and L. Haimberger, 2010: Comments on “Reanalyses suitable for characterizing long-term trends”. *Bull. Amer. Meteor. Soc.*, 10.1175/2010BAMS3070.1.
- Derber, J. C., and W.-S. Wu, 1998: The use of TOVS cloud-cleared radiances in the NCEP SSI Analysis System. *Mon. Wea. Rev.*, **126**, 2287–2299.
- Derber, J. C., R. J. Purser, W.-S. Wu, R. Treadon, M. Poncica, D. Parrish, and D. Kleist, 2003: Flow-dependent Jb in a global grid-point 3D-Var. *Proc. ECMWF annual seminar on recent developments in data assimilation for atmosphere and ocean*. Reading, UK, 8–12 Sept. 2003.
- Desroziers, G., L. Berre, B. Chapnik, and P. Poli, 2005: Diagnosis of observation, background and analysis-error statistics in observation space. *Q. J. R. Meteorol. Soc.*, **131**, 3385–3396.
- Ferraro, R. R., N. C. Grody, F. Weng, and A. Basist, 1996: An eight-year (1987–1994) time series of rainfall, clouds, water vapor, snow cover, and sea ice derived from SSM/I measurements. *Bull. Amer. Meteor. Soc.*, **77**, 891–905.
- Garcia, R.R. and B.A. Boville, 1994: Downward control of the mean meridional circulation and temperature distribution of the polar winter stratosphere, *J. Atmos. Sci.*, **51**, 2238–2245.
- Gaspari, G., S. E. Cohn, J. Guo, and S. Pawson, 2006: Construction and Application of Covariance Functions with Variable Length Fields. *Q. J. R. Meteorol. Soc.*, **132**, 1815–1838.
- Haimberger, L., 2007: Homogenization of radiosonde temperature time series using innovation statistics. *J. Clim.*, **20**, 1377–1403.
- Han, Y., P. van Delst, Q. Liu, F. Weng, B. Yan, R. Treadon and J. Derber, 2006: JCSDA Community Radiative Transfer Model (CRTM) - Version 1, *NOAA Tech Report 122*, 33 pp.
- Hollingsworth, A., and P. Lönnberg, 1989: The verification of objective analyses: Diagnostics of analysis system performance. *Meteorol. Atmos. Phys.*, **40**, 3–27.
- Kalnay, E., and Coauthors, 1996: The NCEP/NCAR 40-year reanalysis project. *Bull. Am. Meteorol. Soc.*, **77**, 437–471.

- Kobayashi, S., M. Matricardi, D. Dee, and S. Uppala, 2009: Toward a consistent reanalysis of the upper stratosphere based on radiance measurements from SSU and AMSU-A. *Q. J. R. Meteorol. Soc.*, **135**, 2086–2099.
- Koster, R. D., M. J. Suárez, A. Ducharme, M. Stieglitz, and P. Kumar, 2000: A catchment-based approach to modeling land surface processes in a GCM, Part 1, Model Structure. *J. Geophys. Res.*, **105**, 24809-24822.
- Kummerow, C., Y. Hong, W. S. Olson, S. Yang, R. F. Adler, J. McCollum, R. Ferraro, G. Petty, D.-B. Shin, and T. T. Wilheit, 2001: The evolution of the Goddard Profiling Algorithm (GPROF) for rainfall estimation from passive microwave sensors, *J. Appl. Meteor.*, **40**, 1801-1820.
- Lin, S.-J., 2004: A vertically Lagrangian finite-volume dynamical core for global models. *Mon. Wea. Rev.*, **132**, 2293-2307.
- Lock, A. P., A. R. Brown, M. R. Bush, G. M. Martin, and R. N. B. Smith, 2000: A new boundary layer mixing scheme. Part I: Scheme description and single-column model tests. *Mon. Wea. Rev.*, **138**, 3187-3199.
- Louis, J., M. Tiedtke, and J. Geleyn, 1982: A short history of the PBL parameterization at ECMWF. *Proc. ECMWF Workshop on Planetary Boundary Layer Parameterization*, Reading, United Kingdom, ECMWF, 59–80.
- McFarlane, N. A., 1987: The effect of orographically excited gravity wave drag on the general circulation of the lower stratosphere and troposphere. *J. Atmos. Sci.*, **44**, 1775-1800.
- Manney, G. L., W. H. Daffer, K. B. Strawbridge, K. A. Walker, C. D. Boone, P. F. Bernath, T. Kerzenmacher, M. J. Schwartz, K. Strong, R. J. Sica, K. Krüger, H. C. Pumphrey, A. Lambert, M. L. Santee, N. J. Livesey, E. E. Remsberg, M. G. Mlynczak, and J. R. Russell III, 2008a: The high Arctic in extreme winters: vortex, temperature, and MLS and ACE-FTS trace gas evolution. *Atmos. Chem. Phys.*, **8**, 505–522.
- Manney, G. L., K. Krüger, S. Pawson, K. Minschwaner, M. J. Schwartz, W. H. Daffer, N. J. Livesey, M. G. Mlynczak, E. E. Remsberg, J. M. Russell III, and J. W. Waters, 2008b: The evolution of the stratopause during the 2006 major warming: Satellite data and assimilated meteorological analyses. *J. Geophys. Res.*, **113**, D11115, doi:10.1029/2007JD009097.
- Moorthi, S., and M. J. Suarez, 1992: Relaxed Arakawa-Schubert, A Parameterization of Moist Convection for General-Circulation Models. *Mon. Wea. Rev.* **120**, 978-1002.
- Onogi, K., H. Koide, M. Sakamoto, S. Kobayashi, J. Tsutsui, H. Hatsushika, T. Matsumoto, N. Yamazaki, H. Kamahori, K. Takahashi, K. Kato, R. Oyama, T. Ose, S. Kadokura and K. Wada, 2005: JRA-25: Japanese 25-year re-analysis project— progress and status. *Q. J. R. Meteorol. Soc.*, **131**, 3259–3268.
- Pawson, S. and M. Fiorino, 1998a: The Tropical Lower Stratosphere in Atmospheric Reanalyses. Part 1: Thermal Structure and the Annual Cycle. *Clim. Dyn.*, **14**, 631-644.

- Pawson, S. and M. Fiorino, 1998b: The Tropical Lower Stratosphere in Atmospheric Reanalyses. Part 2: The Quasi-Biennial Oscillation. *Clim. Dyn.*, **14**, 645-658.
- Pawson, S., I. Stajner, S. R. Kawa, H. Hayashi, W. Tan, J. E. Nielsen, Z. Zhu, L.-P. Chang, N. J. Livesey, 2007: Stratospheric Transport Using Six-Hour Averaged Winds from a Data Assimilation System. *J. Geophys. Res.*, **112**, D23103. DOI:10.1029/2006JD007673.
- Pawson, S., and Coauthors, 2011: Evaluation of the middle and upper stratosphere in MERRA. *J. Clim.* (submitted to MERRA special collection).
- Purser, R. J., W.-S. Wu, D. F. Parrish, and N. M. Roberts, 2003a: Numerical aspects of the application of recursive filters to variational statistical analysis. Part I: Spatially homogeneous and isotropic Gaussian covariances. *Mon. Wea. Rev.*, **131**, 1524-1535.
- Purser, R. J., W.-S. Wu, D. F. Parrish, and N. M. Roberts, 2003b: Numerical aspects of the application of recursive filters to variational statistical analysis. Part II: Spatially inhomogeneous and anisotropic general covariances. *Mon. Wea. Rev.*, **131**, pp. 1536-1548.
- Randel, W. J., F. Wu, J. M. Russell, A. Roche, and J. W. Waters, 1998: Seasonal cycles and QBO variations in stratospheric CH₄ and H₂O observed in UARS HALOE data. *J. Atmos. Sci.*, **55**, 163-185.
- Redder, C. R., J. K. Luers, and R. E. Eskridge, 2004: Unexplained discontinuity in the U.S. radiosonde temperature data. Part II: Stratosphere. *J. Atmos. Oceanic Technol.*, **21**, 1133–1144.
- Reichle, R. H., R. D. Koster, G. J. M. De Lannoy, B. A. Forman, Q. Liu, S. P. P. Mahanama, and A. Touré, 2011: Assessment and enhancement of MERRA land surface hydrology estimates. *J. Clim.* (submitted to MERRA special collection).
- Reynolds, R. W., N. A. Rayner, T. M. Smith, D. C. Stokes and W. Wang, 2002: An improved in situ and satellite SST analysis for climate. *J. Clim.*, **15**, 1609-1625.
- Rienecker, M. M., and Coauthors, 2008: The GEOS-5 Data Assimilation System – Documentation of Versions 5.0.1 and 5.1.0, and 5.2.0. NASA Technical Report Series on Global Modeling and Data Assimilation, NASA/TM-2008-104606, Vol. 27, 92 pp.
- Rienecker, M. M., and Coauthors, 2011: Atmospheric Reanalyses: Recent Progress and Prospects for the Future. A Report from a Technical Workshop at NASA GSFC, Greenbelt MD, April 2010, NASA/TM-2011-104606 (draft).
- Roberts, J. B., C. A. Clayson, F. R. Robertson, and M. G. Bosilovich, 2011: Characterization of turbulent latent and sensible heat flux exchange between the atmosphere and ocean in MERRA. *J. Clim.* (submitted to MERRA special collection).
- Robertson, F. R., M. G. Bosilovich, J. Chen and T. L. Miller, 2011: The effect of satellite observing system changes on MERRA water and energy fluxes. *J. Clim.* (submitted to MERRA special collection).

- Saha, S., and Coauthors, 2010: The NCEP Climate Forecast System Reanalysis. *Bull. Am. Meteorol. Soc.*, **91**, 1015-1057.
- Schubert, S. D., R. Rood, and J. Pfaendner, 1993: An assimilated dataset for earth science applications. *Bull. Am. Meteorol. Soc.*, **74**, 2331-2342.
- Schubert, S., D. Dee, S. Uppala, J. Woollen, J. Bates, and S. Worley, 2006: *Workshop Report: The Development of Improved Observational Datasets for Reanalysis: Lessons Learned and Future Directions*. University of Maryland Conference Center, College Park, MD, 28-29 September 2005, 31 pp. [Available at <http://gmao.gsfc.nasa.gov/pubs/docs/Schubert273.pdf>]
- Schubert, S. D., H. Wang, and M.J. Suarez, 2011: Warm season subseasonal variability and climate extremes in the Northern Hemisphere: The role of stationary Rossby waves. *J. Clim.* (submitted to MERRA special collection).
- Shine, K. P., J. J. Barnett, and W. J. Randel, 2008: Temperature trends derived from Stratospheric Sounding Unit radiances: The effect of increasing CO₂ on the weighting function, *Geophys. Res. Lett.*, **35**, L02710, doi:10.1029/2007GL032218.
- Thorne, P.W., and R.S. Vose, 2010: Reanalyses suitable for characterizing long-term trends. Are they really achievable? *Bull. Am. Meteorol. Soc.*, **91**, 353-361, doi:10.1175/2009BAMS2858.1
- Treadon, R. E., H.-L. Pan, W.-S. Wu, Y. Lin, W. S. Olson, and R. J. Kuligowski, 2002: Global and Regional Moisture Analyses at NCEP. *Proc. ECMWF/GEWEX Workshop on Humidity Analysis*, 8-11 July 2002, 33-47.
- Uppala, S.M., and Coauthors, 2005: The ERA-40 re-analysis. *Q. J. R. Meteorol. Soc.* **131**, 2961–3012.
- Wentz F. J., 1997: A well-calibrated ocean algorithm for SSM/I. *J. Geophys. Res.*, **102**, 8703-8718.
- Wu, W.-S., R. J. Purser and D. F. Parrish, 2002: Three-dimensional variational analysis with spatially inhomogeneous covariances. *Mon. Wea. Rev.*, **130**, 2905-2916.
- Xie P., and P. A. Arkin, 1996: Global precipitation: A 17-year monthly analysis based on gauge observations, satellite estimates, and numerical model outputs. *Bull. Amer. Meteor. Soc.*, **78**, 2539-2558.
- Yi, Y., J. S. Kimball, L. A. Jones, R. H. Reichle, and K. C. McDonald, 2011: Evaluation of MERRA land surface estimates in preparation for the Soil Moisture Active Passive mission. *J. Clim.* (submitted to MERRA special collection).
- Zou, C., M. D. Goldberg, Z. Cheng, N. C. Grody, J. T. Sullivan, C. Cao, and D. Tarpley, 2006: Recalibration of microwave sounding unit for climate studies using simultaneous nadir overpasses. *J. Geophys. Res.*, **111**, D19114, doi:10.1029/2005JD006798